AD-A067 237 ROYAL AIRCRAFT ESTABLISHMENT FARNBOROUGH (ENGLAND) F/G 22/3
DETERMINATION AND GEOPHYSICAL INTERPRETATION OF THE ORBIT OF CH--ETC(U)
AUG 78 H HILLER
UNCLASSIFIED RAE-TR-78107 DRIC-BR-66747 NL

1 OF 1
ADA
067237

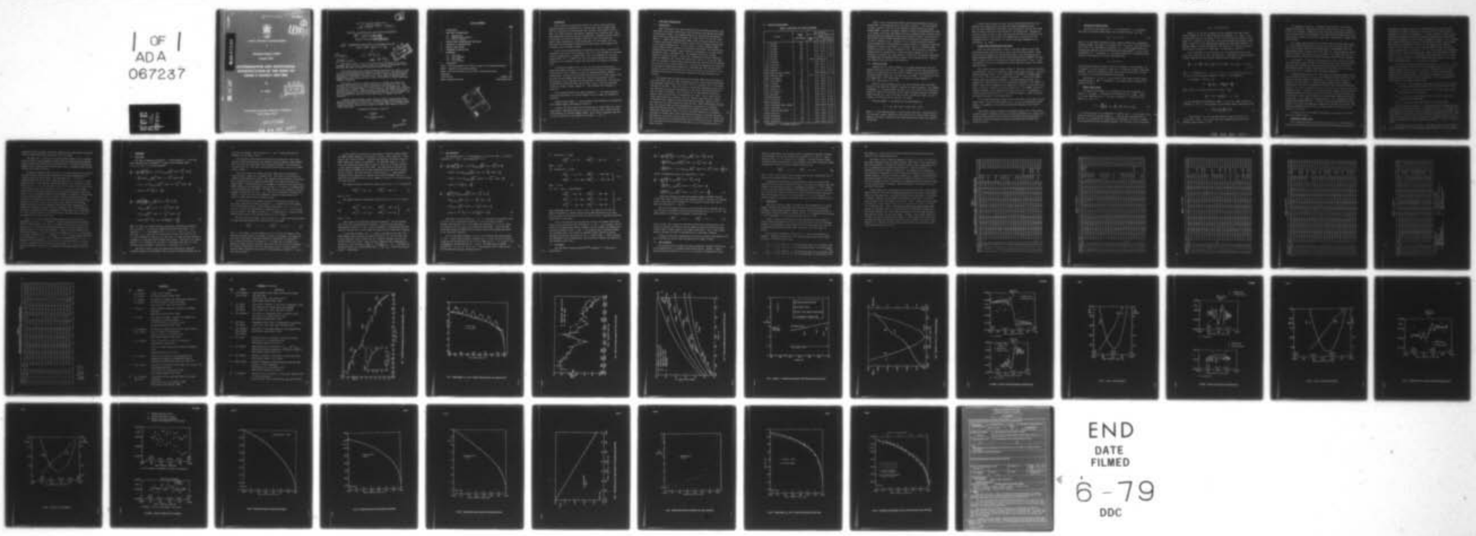

END
DATE
FILMED
6-79
DDC

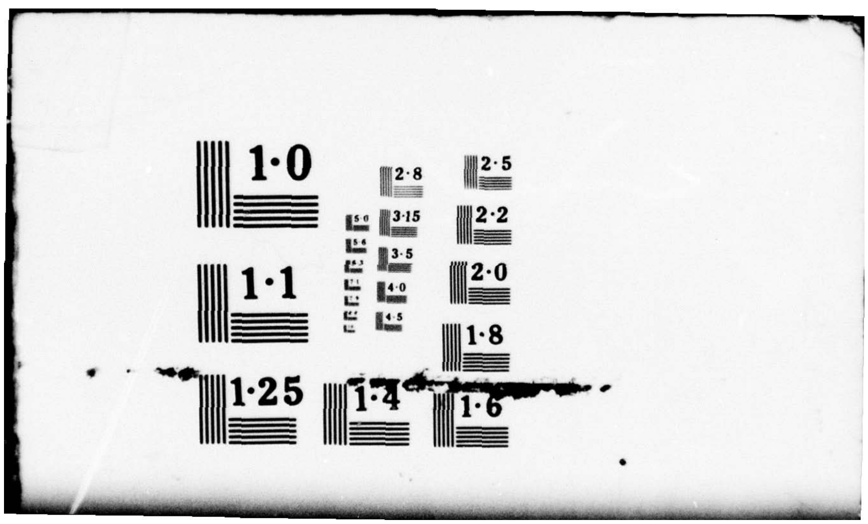
1·0
2·8
2·5
3·15
2·2
3·5
2·0
4·0
1·1
4·5
1·8
1·25
1·4
1·6

BR66747

UNLIMITED

TR 78107

TR 78107

LEVEL II

ROYAL AIRCRAFT ESTABLISHMENT

*

Technical Report 78107

August 1978

DETERMINATION AND GEOPHYSICAL INTERPRETATION OF THE ORBIT OF CHINA 2 ROCKET (1971-18B)

by

H. Hiller

*

Procurement Executive, Ministry of Defence
Farnborough, Hants

UNLIMITED

(2)

UDC 521.6 : 521.3 : 629.19.077.3

(14) RAE-TR-78107

ROYAL AIRCRAFT ESTABLISHMENT

(9) Technical Report ~~78107~~

(11)

Received for printing ~~31~~ Aug~~ust~~ ~~19~~78

(6) DETERMINATION AND GEOPHYSICAL INTERPRETATION OF THE ORBIT OF CHINA 2 ROCKET (1971-18B).

by

(10) H. Hiller

(18) DRIC

(19) BR-66747

(12) 50p.

SUMMARY

The orbit of China 2 rocket, 1971-18B, has been determined at 114 epochs throughout its 5-year life, using the RAE orbit refinement program PROP 6, with more than 7000 radar and optical observations from 83 stations.

The rocket passed slowly enough through the resonances 14:1, 29:2, 15:1 and 31:2 to allow lumped geopotential harmonic coefficients to be calculated for each resonance, by least-squares fittings of theoretical curves to the perturbation-free values of inclination and eccentricity. These lumped coefficients can be combined with values from satellites at other inclinations, to obtain individual harmonic coefficients.

The rotation rate of the upper atmosphere, at heights near 300 km, was estimated from the decrease in orbital inclination, and values of 1.15, 1.05, 1.10 and 1.05 rev/day were obtained between April 1971 and January 1976. From the variation in perigee height, 25 values of density scale height were calculated, from April 1971 to decay. Comparison with values from the COSPAR International Reference Atmosphere 1972 shows good agreement between April 1971 and October 1975, but the observational values are 10 per cent lower, on average, than *CIRA* thereafter.

A further 1400 observations, made during the final 15 days before decay, were used to determine 15 daily orbits. Analysis of these orbits reveals a very strong west-to-east wind, of 240 ± 40 m/s, at a mean height of 195 km under winter evening conditions, and gives daily values of density scale height in the last 7 days before decay.

Departmental Reference: Space 557

310450

LIST OF CONTENTS

1 INTRODUCTION

China 2 rocket was launched on 3 March 1971 into an orbit having the following elements: inclination 69.9^o, perigee height 265 km, apogee height 1825 km, eccentricity 0.105 and period 106.1 minutes. After nearly 5 years in orbit, the rocket decayed in the Earth's atmosphere on 16 February 1976. Over 7000 observations have been used with the RAE orbit refinement program[1], PROP 6, to determine 114 orbits, 40 of which contained at least one sequence of Hewitt-camera observations. Orbits between July 1971 and January 1972 have previously been determined[2] by Brookes and Ryland, mostly with slightly lower accuracies, for air-density studies.

As the orbit contracted under the influence of air drag, it passed first through the tail-end of 27:2 resonance in April 1971, then through 14:1 resonance (when the ground track is repeated daily, every 14 revolutions of the orbit) during October 1972. In March 1974, the orbit passed through 29:2 resonance, followed by 15:1 resonance in March 1975, and then 31:2 resonance in November 1975.

An analysis was made of each of the four resonances specified above, using least-squares fittings to the perturbation-free values of inclination and eccentricity for each resonance, to give the lumped geopotential harmonic coefficients. Although the coefficients obtained are not of high accuracy, they may still be good enough, when used with values from satellites at other inclinations, to give improved individual harmonic coefficients. The variation of inclination during the whole life is shown in Fig 1, with the variations during the resonant regions 'mapped in'. The resonances are discussed in section 7.

The rotational speed of the upper atmosphere, Λ , has been determined between the resonances, for various heights and local times, as discussed in section 6.

Density scale height, H , was calculated from variations in perturbation-free perigee height, as discussed in section 5.

Finally, when this study was near completion, a further 3000 or so radar observations, made during the final 15 days of orbital life, arrived from the North American Air Defense Command, NORAD. Daily orbits, determined from 1400 of these observations, were analysed to determine Λ and H .

2 MAIN ORBIT DETERMINATION

2.1 Observations

About 7500 optical and radar observations were available initially, from which about 450 US Navy observations, with elevations below 20°, were discarded as being less reliable. The remaining 7000 or so were distributed among 114 orbits which were determined throughout the 5-year orbital life of the rocket (Table 1). Almost 1500 observations (about 20 per cent) were rejected as ill-fitting, leaving about 5560 observation (49 per orbit on average) actually used in the orbital determinations. Forty of these 114 orbits contained highly accurate Hewitt-camera sequences of observations (with about four observations selected from each sequence), made at Malvern or Edinburgh: 31 of these orbits had Malvern only; 7, Edinburgh only. The remaining two orbits included sequences from both stations. Nine of the 31 Malvern-only orbits contained at least two sequences, one of which was rejected for orbits 31, 32 and 38. Only orbit 29 contained a single Malvern sequence which was rejected but, fortunately, the orbit was fairly accurate without it. This rejected sequence was at the end of the group of observations being used to determine the orbit and, in such a situation, rejection occasionally does occur, not because of any defects in the observations but because of irregular variations in air drag that spoil the fitting.

The largest group of observations used was about 2800 from the US Navy, of which only about 8 per cent were ultimately rejected. British radar observations were available almost daily from 22 April 1975 to 15 February 1976 (*ie* the final 300 days of the life). Since there were on average four sequences per day, only one observation per sequence was selected so that these observations would not have too great an influence. This resulted in 1225 observations distributed among 34 orbits, giving about 36 observations per orbit. About 15 per cent of these observations were ultimately rejected. Malvern radar supplied a further 51 sequences, with a mean of three observations per sequence, during 1971-73, but nearly half of these observations were rejected. Other observations available were 136 from the South African kinetheodolite (43 rejected); 115 sequences comprising 380 observations (23 rejected) from Jokioinen, Finland; and about 2180 visual observations (about 25 per cent rejected) supplied by the Appleton 107
Laboratory at Slough. These visual observations were made by volunteer observers, predominantly in Britain, with stations 2414 (D.J. Hopkins), 2420 (R.D. Eberst) and 2421 (D.M. Brierley) all contributing more than 250 observations each. There were also observations from South Africa, Australia, Cyprus, the Netherlands and ten other countries.

2.2 Observational accuracy

Table 2 - Residuals for selected stations

Station		Number of observations	Rms residuals			
			Range km	Minutes of arc		
				RA	Dec	Total
1	US Navy	243		1.6	1.9	2.5
2	US Navy	63		1.4	1.8	2.3
3	US Navy	48		1.7	1.4	2.2
4	US Navy	62		1.8	1.4	2.3
5	US Navy	175		1.7	1.7	2.4
6	US Navy	195		1.6	1.7	2.3
29	US Navy	1775	0.6*	0.25*	0.4*	
414	Capetown	74		2.9	3.0	4.1
616	Adelaide 5	13		0.9	1.4	1.7
2152	Akrotiri 2	11		1.5	2.5	2.9
2265	Farnham	43		2.2	2.4	3.3
2303	Malvern Hewitt Camera	134		0.03	0.04	0.05
2304	Malvern radar	71	0.9	2.4	2.4	
2402	Stevenage 2	16		1.8	1.9	2.6
2414	Bournemouth	367		4.1	3.6	5.5
2419	Tremadoc	96		2.8	2.4	3.7
2420	Willowbrae	353		2.1	2.2	3.0
2421	Malvern 4	278		2.0	1.9	2.7
2430	Stevenage 4	16		1.0	1.7	2.0
2432	Horsham	15		2.0	1.7	2.7
2437**	Warrington	10		7.6	2.1	7.9
2513	Colchester	17		4.0	2.4	4.6
2528	Aldershot	12		1.4	1.4	1.9
2534	Edinburgh Hewitt Camera	36		0.04	0.03	0.05
2539	Dymchurch	13		1.4	1.4	2.0
2577	Cape Kinetheodolite	93		0.7	0.8	1.1
2596	Akrotiri	20		2.7	3.8	4.7
4126	Gröningen	14		2.9	3.3	4.4
6702	Jokioinen	357		3.4	3.4	4.8
8597	Adelaide 4	19		2.4	3.9	4.5

107

* Geocentric ** includes station 47

Table 2 lists the observing stations which have contributed at least ten observations to the determination of the orbits in Table 1. The observational accuracy is given in the form of rms residuals, obtained using the computer program ORES[3]. As usual, the Hewitt cameras at Malvern and Edinburgh (the latter is no longer in use) have the highest accuracy, averaging around 3 seconds of arc. The South African kinetheodolite had a mean residual of about 1.1 minutes of arc. The US Navy stations showed remarkably uniform topocentric accuracies, between 2.2 and 2.5 minutes of arc. (Station 29 is a fictitious geocentric station whose residuals must be multiplied by a factor of about 5 to obtain an equivalent topocentric accuracy, which comes to 2.3 minutes of arc.) The Malvern radar yielded an accuracy of about 3.4 minutes of arc. The theodolite at Jokioinen, Finland was up to standard with a little less than 5 minutes of arc. The remaining 18 stations, all visual observers reporting to the Appleton Laboratory at Slough, have rms residuals mostly between 2 and 5 minutes of arc. Lists of the residuals have been sent to the observers.

2.3 Orbital accuracy

Computed sets of orbital elements at 114 epochs between April 1971 and February 1976 are listed in Table 1, with standard deviations where appropriate. The sd in inclination varies from 0.0003 to 0.0026°, the rms being 0.0012°; for the Hewitt-camera orbits only, the rms value was 0.0008°. For eccentricity, the sd varies from 3×10^{-6} (equivalent to 22 metres in perigee height) to 44×10^{-6}, with an rms of 15×10^{-6}.

The sd in right ascension of the node varies between 0.001° and 0.002°, except for the final orbit (0.004°), showing very good consistency. The argument of perigee, ω, and mean anomaly at epoch, M_0, have similar sd, varying from 0.003° to 0.016° for the first 64 orbits; then increasing, generally to between 0.02° and 0.04° up to orbit 102; then to 0.05° to 0.08° up to orbit 112; and finally to 0.13° and 0.34° for the last two orbits.

The mean anomaly M is modelled in the PROP program[4] as

$$M = M_0 + M_1 t + M_2 t^2 + M_3 t^3 + M_4 t^4 + M_5 t^5 ,$$

where t is the time from epoch. It can be seen from Table 1 that during 1971 the M_5-term is rarely required; by 1974 about half the orbits require the M_5-term; for the final 12 orbits (in the three months before decay), ten required the M_5-term.

Fifteen orbits contained at least one day during which there was a geomagnetic storm (defined here as having the planetary geomagnetic index $A_p \geqslant 50$), even though (some successful) steps were taken to exclude such stormy days by careful selection of the time-span of the observations. Although the accuracy of some of these 15 orbits may have been affected by the density variations associated with the storms, they compared well in accuracy with the 'stormless' orbits. (The effect of a storm on the upper atmosphere is not indicated by A_p alone.)

3 FURTHER ORBIT DETERMINATIONS NEAR DECAY

After the orbits described in section 2 had been computed, about 3000 observations, made during the last 15 days of the life, were received. These were made by the assigned and contributing sensors of the North American Air Defense Command (NORAD) Space Detection and Tracking System (SPADATS), and about 1400 of them were used to determine daily orbits during these 15 days. It was not possible to use all the observations because PROP only accepts 100 observations per epoch.

The 15 daily orbits are listed in Table 3. They are of excellent accuracy and consistency. The sd in inclination varies from 0.0007 to 0.0011°. The sd in eccentricity varies from 7×10^{-6} (equivalent to 50 metres in perigee height) to 17×10^{-6}. The sd in right ascension of the node Ω varies from 0.0006 to 0.0015°, while the argument of perigee ω and mean anomaly at epoch, M_0, (generally of similar accuracy) have sd between 0.04 and 0.40°. The elements in Tables 1 and 3 can be compared for the same epoch, *ie* orbit 113 with orbit C and orbit 114 with K. On orbits 113 and 114, the sd in e is 0.00004, and this is reduced to 0.00001 on the one-day orbits, while the sd in i is reduced by a factor of about 2½ and the sd in Ω by a factor of about 3. These illustrate the improved accuracy of the one-day orbits.

It is worth noting that the epoch of the final orbit is only about 2 hours before decay. This is why the values of $M_2 - M_4$ are so exceptionally large. However, the imminence of decay did not affect the accuracy of the orbital elements.

The orbital elements of Table 3 are plotted in Figs 14-18. These orbits are more accurate and frequent than any previously published, for a time so near decay, and their analysis gives values of scale height and upper-atmosphere winds with a finer time resolution than has previously been possible (see sections 5 and 6).

4 VARIATION IN PERIGEE HEIGHT

The values of semi major axis, a, and eccentricity, e, from Table 1 were used to calculate perigee height over a spherical Earth, h_p, from

$$h_p = a(1 - e) - R \, , \tag{1}$$

where R is the Earth's equatorial radius, taken as 6378.16 km, as assumed in the PROP program. The values are plotted in Fig 2 as circles. The main oscillation is due to the odd-harmonic perturbation in e, which, combined with the lunisolar perturbation, was calculated using the PROD program[4], to give a total perturbation Δe. A parameter Q, the perigee height over a spherical Earth, cleared of perturbations, can now be determined from

$$Q = h_p + a\Delta e \, ,$$

and the values obtained are shown in Fig 2 by triangles. The perturbation Δe is assumed to be zero initially, so that the Q values are relative rather than absolute. This is not significant here, since only the slope dQ/dt is used (in section 5) for calculating density scale height.

The values of h_p and Q, in the final 15 days before satellite decay, calculated using a and e from Table 3, are plotted in Fig 19, which is an extension of Fig 2.

5 DENSITY SCALE HEIGHT

The density scale height H is a measure of the rate of decrease of density ρ as height y increases, and is defined by $\frac{1}{H} = -\frac{1}{\rho}\frac{d\rho}{dy}$. Values of H were calculated from $\dot{Q}$, the rate of change of Q due to air drag, where[5], for $ae/H > 3$,

$$\dot{Q} = -\frac{2HM_2}{3M_1 e}\left(1 - 2e + \frac{H}{4ae} - \frac{2\varepsilon'}{e}\sin^2 i \cos 2\omega\right) , \tag{2}$$

ε' is the ellipticity of the atmosphere ($= 0.00335$) and H is at a height $1.5\,H_p$ 107
above the satellite's perigee height y_p. Ignoring small perturbations, we may take y_p as given by the right-hand side of equation (1) with R replaced by the local Earth radius at perigee latitude. For 1971-18B, at 70° inclination,

$$y_p = h_p + 18.8 \sin^2 \omega \ .$$

Values of $\dot{Q}$ for use in equation (2) are obtained in the form $\Delta Q/\Delta t$, from the change ΔQ in Q over a suitable time interval Δt. Since Q has an accuracy of about 0.1 km, values of ΔQ of 3 km or more are required to give values of $\dot{Q}$ accurate to 3 per cent, and the time intervals were chosen on this basis. Values of H were obtained from equation (2) using these values of $\dot{Q}$ and mean values of the other parameters. The values of H are plotted against time in Fig 3 as circles, up to MJD 42770. At this point, $ae/H \triangleq 3$.

In the remainder of the calculations for H, from MJD 42770 to the end of the life, the value of ae/H was less than 3. The 'phase 2' regime discussed in Ref 6 (page 88) can then be used: equation (5.35) of Ref 6 gives

$$\frac{da}{dx} = y_0 + \tfrac{1}{2}e\left(4 - 3y_0^2 - y_0 y_2\right) - \tfrac{1}{2}c \cos 2\omega(y_0 - 2y_2 + y_0 y_3) = \beta \text{ , say,} \qquad \ldots\ldots(3)$$

where $c = \dfrac{\varepsilon' a(1 - e)}{2H} \sin^2 i$, $y_r = I_r/I_1$, and I_r is the Bessel function of the first kind and imaginary argument, of order r (*ibid*, page 36).

To calculate H from $\dot{Q}$, put

$$\dot{Q} = \frac{dQ}{da} \cdot \frac{da}{dt} = -\frac{d(a - x)}{da} \cdot \frac{2\dot{n}a}{3n} ,$$

where $n(= M_1)$ is the mean motion and $\dot{n} = 2M_2$. Hence

$$\frac{da}{dx} = 1\Big/(1 + 3M_1\dot{Q}/4M_2 a) = \alpha \text{ , say.} \qquad (4)$$

H is now determined by guessing two values, H_1 and H_2, which are used to calculate β_1 and β_2 from equation (3), and then by linear interpolation from

$$H = \frac{H_1(\beta_2 - \alpha) + H_2(\alpha - \beta_1)}{\beta_2 - \beta_1} \ . \qquad (5)$$

These values of H have also been plotted in Fig 3 as circles, for $42770 < \text{MJD} < 42824$. The sd shown have been estimated from the errors in

107 perigee height (usually 0.1 km).

For comparison, values of H obtained[7] from *CIRA 1972*, for the same heights and exospheric temperatures as the calculated values, are also plotted in Fig 3, as triangles. Consecutive points have been joined (where possible) to give an overall view of the difference. To avoid confusion between some of the points, only one half of the sd-bar is shown where overlap with a triangle would have occurred.

Fig 3 shows that from April 1971 to October 1975 the observational values of H , for heights between 250 and 350 km, are generally within 10 per cent of the *CIRA 1972* values and have the same mean value. From November 1975, the observational values are mostly lower than *CIRA 1972*. Since atmospheric density varies so widely - by a factor up to 5 at 300 km - Fig 3 shows that *CIRA 1972*, which incorporates Jacchia's 1971 model[8], provides a good reference atmosphere.

Ten values of H obtained from equations (3) to (5), using the 15 daily orbits near decay (given in Table 3), are also plotted in Fig 3 for MJD between 42810 and 42824; during this time the height falls from 260 to 205 km. The observational values are mostly lower than those from *CIRA 1972*, on average by about 10 per cent, a difference that is probably significant.

The observational values of H have been plotted against height in Fig 4; they are shown as crosses or circles, and comparative curves from *CIRA 1972* are given, for various exospheric temperatures. The observational values are numbered 1-25, with points 1-15 having bracketed numbers giving exospheric temperatures, corrected for semi-annual variation[9], which have been calculated[7] using *CIRA 1972* with the appropriate values of solar 10.7 cm radiation energy and geomagnetic index. For points 1-7, the local time at perigee is used in calculating the temperature; but for points 8-15, local time is averaged, because the eccentricity is lower, and the position on the orbit where drag has most effect in altering Q (at a height 1.5 H above perigee) is at a considerable angular distance from perigee (60° when $e = 0.02$), so that the appropriate local time required is not that at perigee but averaged over a wide arc of the orbit. The bracketed temperatures given in Fig 4 are those used in calculating the *CIRA* values of H in Fig 3.

For points 16-25, the exospheric temperatures are between 770 and 810 K and are not shown on Fig 4.

6 ATMOSPHERIC ROTATION RATE

The 114 derived values of inclination, given in Table 1, were cleared of lunisolar and geopotential perturbations using the PROD program[4] with numerical

integration at one-day intervals. The modified values are plotted in Fig 1. The theoretical change in inclination was calculated for several values of atmospheric rotation rate (expressed as Λ times the Earth's rotation rate), using oblate-atmosphere theory[10], with numerical integration at about 18-day intervals (corresponding to 22.5° steps in argument of perigee). The 114 points were considered in groups separated by the resonance regions. (These regions were filled, as explained in section 7, by the resonance oscillations.) Orbits 1-37 were taken as the first group (MJD 41068 to 41547) and the best fitting, shown in Fig 1, is given by $\Lambda = 1.15 \pm 0.05$ rev/day, at a mean height $\bar{y} = \bar{y}_p + 0.75H = 315$ km; the second group, orbits 42-61 (MJD 41665 to 42028), gives $\Lambda = 1.05 \pm 0.05$ at $y = 310$ km; the third group gives $\Lambda = 1.10 \pm 0.05$ for $y = 295$ km, for orbits 65-76 (MJD 42181-42413); and fourthly, for orbits 82-112 (MJD 42533-42798), $\Lambda = 1.05 \pm 0.05$ at $y = 270$ km.

It is known[11] that the zonal wind speed depends on local time, Λ being greater in the evening (18-24 h) than in the morning (04-12 h): so the local time at perigee is plotted at the top of Fig 1. The fitting of the first group of points reveals no bias in local time, *ie* evening and morning were sampled equally (mean conditions). The second fitting shows a slight morning bias; the third and fourth fittings are unbiased. So the results from the four fittings can be summarised as follows:

(1) $\Lambda = 1.15 \pm 0.05$, implying a west-to-east wind of 60 ± 20 m/s, under mean (evening and morning) conditions, at a mean height of 315 km.

(2) $\Lambda = 1.05 \pm 0.05$ (west-to-east wind of 20 ± 20 m/s), with a slight morning bias, at 310 km height.

(3) $\Lambda = 1.10 \pm 0.05$ (west-to-east wind of 40 ± 20 m/s), under mean conditions, at 295 km height.

(4) $\Lambda = 1.05 \pm 0.05$, under mean conditions, at 270 km height.

The sd in the above values of Λ are obtained from the estimated accuracy of fitting the curve to the values of inclination in Fig 1. For example, the first group are fitted with an accuracy estimated as slightly better than 0.001°, say 0.0008° (of the 36 points, none is more than 0.0025° from the curve). This error is just under 5 per cent of the decrease in inclination over the first group of points, giving a similar proportional error in Λ, that is an error of 0.05.

In calculating the curves of Fig 1, meridional winds have been ignored:
107 they are unlikely to have an appreciable effect because (a) the local time is

averaged over day and night, and (b) the satellite has a high orbital inclination (70^o), for which meridional wind effects tend to be small.

The values of Λ , with sd, are plotted against height in Fig 5, together with the curves of mean atmospheric rotation rate, and morning and evening wind speeds, derived from analysis of 31 previous orbits[11]. The values obtained here suggest that the average curve should be rather lower at heights between 260 and 300 km, for the years 1971-1975.

In the inset diagram on the left of Fig 1, the final two values of inclination from the main curve have been replaced by the values obtained from the 15 daily orbits just before decay. The curve shown has $\Lambda = 1.05$ up to 5 February 1976: but for the last 11 days the value is $\Lambda = 1.6 \pm 0.1$, at a mean height of 195 km. This implies a west-to-east wind of 240 ± 40 m/s at a local time of 19-23 h. It is well established (see Ref 11) that the west-to-east winds are strongest during the evening hours, 18-24 h, but 240 m/s is the highest reliable value of wind speed that has been obtained from analysis of satellite orbits. This is presumably because 1971-18B happened to sample the evening winds at their strongest during its last few days in orbit, and because the daily orbits allow an analysis over a much shorter time span than has generally been possible in the past. West-to-east winds of up to 300 m/s at the evening maximum in winter have been recorded by radar back-scatter measurements[12] at heights near 200 km at latitude 47^o north in February 1970. These conditions are closely comparable with those experienced by the perigee of 1971-18B during its last 11 days in orbit (6 to 16 February 1976), when the perigee latitude increased from 15^o north to 50^o north.

The $\Lambda = 1.6$ curve has been plotted (unbroken line) in Fig 20, with a comparative curve for $\Lambda = 1.4$ (dashed). To assess the influence of meridional winds[13] (south-to-north), the effect of a 200 m/s south-to-north wind (a rotation rate $\mu = 0.4$ rev/day) has been calculated and is shown in Fig 20 by the dash-dot curve. It is seen that changing μ from 0 to 0.4 has slightly less effect than changing Λ from 1.4 to 1.6; so a change of 0.1 in Λ is equivalent to a change of about 0.3 in μ . Thus the $\Lambda = 1.6$; $\mu = 0$ curve might be replaced by the alternative $\Lambda = 1.5$; $\mu = 0.3$. However, a meridional wind of $\mu = 0.3$ (150 m/s) is most unlikely at local time 19-23 h, when such winds are usually slight[14], averaging less than 50 m/s: so the estimate of $\Lambda = 1.6 \pm 0.1$ rev/day can stand unaltered, any effects of meridional winds being absorbed in the 0.1 error.

7 RESONANCES

7.1 14th order

The rates of change of inclination i and eccentricity e near 14th-order resonance may be expressed[15], in terms of the resonance angle $\Phi = \omega + M + 14(\Omega - \nu)$, by the equations:

$$\begin{aligned}\frac{di}{dt} = \frac{n}{\sin i}\left(\frac{R}{a}\right)^{14}\Bigg[&\frac{R}{a}(14 - \cos i)\bar{F}_{15,14,7}\left\{\bar{S}_{14}^{0,1}\sin\Phi + \bar{C}_{14}^{0,1}\cos\Phi\right\}\\ &+ \frac{15e}{2}(14)\bar{F}_{14,14,7}\left\{\bar{C}_{14}^{1,0}\sin(\Phi - \omega) - \bar{S}_{14}^{1,0}\cos(\Phi - \omega)\right\}\\ &+ 11e(7 - \cos i)\bar{F}_{14,14,6}\left\{\bar{C}_{14}^{-1,2}\sin(\Phi + \omega) - \bar{S}_{14}^{-1,2}\cos(\Phi + \omega)\right\}\\ &+ \text{terms in } e^{|q|}\begin{matrix}\cos\\ \sin\end{matrix}(\gamma\Phi - q\omega)\Bigg] ;\end{aligned} \tag{6}$$

$$\begin{aligned}\frac{de}{dt} = \frac{n}{2}\left(\frac{R}{a}\right)^{14}\Bigg[&e\left(\frac{R}{a}\right)\bar{F}_{15,14,7}\left(\bar{S}_{14}^{0,1}\sin\Phi + \bar{C}_{14}^{0,1}\cos\Phi\right)\\ &- 15\bar{F}_{14,14,7}\left\{\bar{C}_{14}^{1,0}\sin(\Phi - \omega) - \bar{S}_{14}^{1,0}\cos(\Phi - \omega)\right\}\\ &+ 11\bar{F}_{14,14,6}\left\{\bar{C}_{14}^{-1,2}\sin(\Phi + \omega) - \bar{S}_{14}^{-1,2}\cos(\Phi + \omega)\right\}\\ &+ \text{terms in}\left[e^{|q|-1}\left\{q - \tfrac{1}{2}(k + q)e^2\right\}\begin{matrix}\cos\\ \sin\end{matrix}(\gamma\Phi - q\omega)\right]\Bigg] .\end{aligned} \tag{7}$$

$\bar{C}_{14}^{q,k}$ and $\bar{S}_{14}^{q,k}$ are lumped 14th-order geopotential coefficients, defined in Ref 15, and the $\bar{F}$ are Allan's normalized inclination functions[16]. The quantities γ, q are integers, with $\gamma = 1, 2, 3 \ldots$ and $q = 0, \pm1, \pm2 \ldots$. The value $\gamma = 2$ is associated with geopotential harmonics of order 28, and $\gamma = 3$ with harmonics of order 42, etc; only the $\gamma = 1$ terms have been used here, although $\gamma = 2$ terms were tried (without much success). The value $q = 2$ leads to terms in e^2 in equation (6), and since $e = 0.08$ here, only the $q = 0$ and ±1 terms have been considered. The suffix k is given by $k = \gamma - q$.

The orbit of China 2 rocket was appreciably perturbed by 14th-order resonance between July and December 1972, and exact 14th-order resonance ($\dot{\Phi} = 0$)

occurred on 14 October. The variations of Φ and $\dot{\Phi}$ between May 1972 and February 1973 are shown in Fig 6.

The variations in inclination and eccentricity during this time, after removal of other perturbations, were analysed using the computer program THROE[17], which fits the values with numerically-integrated versions of the equations of the form (6) or (7). The orbits used include US Navy orbits as well as the PROP orbits of Table 1.

The final inclination fittings utilized 7 PROP values and 10 US Navy values between 11 August and 14 December 1972. The values of inclination were cleared of perturbations as follows. The lunisolar and odd harmonic perturbations were calculated using the computer program PROD[4], the combined maximum value being 0.0052°. The perturbation due to atmospheric rotation was calculated within THROE, assuming a mean atmospheric rotation rate of 1.1 rev/day, the maximum value of the perturbation being 0.0068°. The PROP values were also cleared of tesseral harmonic perturbations due to the $J_{2,2}$ term in the geopotential (maximum value 0.0016°). The US Navy values were assigned a uniform standard deviation of 0.003°; the PROP values had the sd given in Table 1.

In the analysis of the resonant variation in inclination, various (γ,q) pairs were tried, and the number of values of i included was also the subject of a trial-and-error process. After several trials with $(\gamma, q) = (1, 0)$, $(1, 1)$ and $(1, -1)$ in various combinations, it appeared that $(\gamma, q) = (1, 0)$ alone gave the best results. The number of values of i included was not a critical factor. Closely similar results were obtained with 35, 20 or 17 values.

The most favoured fitting, to the 17 values of i, gave the following values of lumped 14th-order geopotential coefficients of odd degree:

$$10^9 \bar{C}_{14}^{0,1} = 32 \pm 11 \quad ; \quad 10^9 \bar{S}_{14}^{0,1} = -2 \pm 20 \tag{8}$$

with $\varepsilon = 0.76$, where ε is the measure of fit (ε^2 = sum of the squares of the weighted residuals divided by the number of degrees of freedom). The values (8) were used in determining individual 14th-order coefficients of odd degree[15]. Fig 7a shows the fitting for 35 values of i (14 PROP plus 21 US Navy): this diagram is shown because it indicates (more fully than the 17-value fitting) how the resonant perturbations fall off on going away from the central resonance, and also shows conclusively that there is a mean decrease of 0.006° in i due to 14th-order resonance.

107

In the analysis of eccentricity, the effects of drag were removed within the THROE program, assuming a scale height H = 50 km. Other values of H were found to give inferior results. Lunisolar perturbations, calculated using the PROD program, were found to be negligible. The nine PROP values of e were given the standard deviations shown in Table 1, while the 11 US Navy values of e were initially assigned an sd of 0.0001. Two other values of sd were also tried (0.0002 and 0.0004) and the value 0.0002 was finally selected as giving the best fitting. This best fitting of the 20 values of e, made using the integrated form of equation (7), between 18 July and 24 December 1972, was shared by two alternative sets of (γ, q), namely $(1, 1)$ and $(1, \pm 1)$, and the fittings are shown in Fig 7b.

The lumped 14th-order coefficients given by the $(\gamma, q) = (1, 1)$ fitting are:-

$$10^9 \bar{C}_{14}^{1,0} = 790 \pm 110 \quad ; \qquad 10^9 \bar{S}_{14}^{1,0} = 400 \pm 20 \tag{9}$$

with $\varepsilon = 1.21$.

The lumped 14th-order coefficients given by the $(\gamma, q) = (1, \pm 1)$ fitting are:

$$\text{and} \quad \left.\begin{aligned} 10^9 \bar{C}_{14}^{1,0} &= 850 \pm 150 \quad ; \qquad 10^9 \bar{S}_{14}^{1,0} = 580 \pm 270 \\ 10^9 \bar{C}_{14}^{-1,2} &= 130 \pm 250 \quad ; \qquad 10^9 \bar{S}_{14}^{-1,2} = 40 \pm 170 \end{aligned}\right\} \tag{10}$$

with $\varepsilon = 1.27$.

These values are considerably larger than expected[15], and the fittings (Fig 7b) are not satisfactory near resonance. In view of this deficiency, a simultaneous fitting of i and e was not attempted. No explanation has been found for the poor fit; at first sight the values in Fig 7b seem quite promising.

It was found necessary, for e, to make a correction in the use of the THROE program, which integrates assuming the value of M_2 for the first orbit of two consecutive orbits, whereas the M_2 should be averaged over the time interval between the orbits. This correction, which has been accomplished by taking M_2 at the nth epoch as $\left[(M_1)_{n+1} - (M_1)_n\right] / 2(t_{n+1} - t_n)$, represents the integrated effect of air drag between times t_n and t_{n+1}. This error does not affect i appreciably.

7.2 29:2 resonance

The resonance angle Φ is now given by $\Phi = 2(\omega + M) + 29(\Omega - \nu)$ and the variations of i and e may be expressed[19] as:

$$\frac{di}{dt} = \frac{n}{\sin i}\left(\frac{R}{a}\right)^{29}\left[\frac{R}{a}(29 - 2\cos i)\bar{F}_{30,29,14}\left\{\bar{S}_{29}^{0,2}\sin\Phi + \bar{C}_{29}^{0,2}\cos\Phi\right\}\right.$$

$$+ 16e(29 - \cos i)\bar{F}_{29,29,14}\left\{\bar{C}_{29}^{-1,1}\sin(\Phi - \omega) - \bar{S}_{29}^{-1,1}\cos(\Phi - \omega)\right\}$$

$$+ 12e(29 - 3\cos i)\bar{F}_{29,29,13}\left\{\bar{C}_{29}^{-1,3}\sin(\Phi + \omega) - \bar{S}_{29}^{-1,3}\cos(\Phi + \omega)\right\}$$

$$\left. + \text{terms in } e^{|q|}\begin{matrix}\cos\\ \sin\end{matrix}(\gamma\Phi - q\omega)\right] \quad ; \tag{11}$$

$$\frac{de}{dt} = n\left(\frac{R}{a}\right)^{29}\left[-\frac{R}{a}\bar{F}_{30,29,14}e\left(\bar{S}_{29}^{0,2}\sin\Phi + \bar{C}_{29}^{0,2}\cos\Phi\right)\right.$$

$$- 16\bar{F}_{29,29,14}\left\{\bar{C}_{29}^{-1,1}\sin(\Phi - \omega) - \bar{S}_{29}^{-1,1}\cos(\Phi - \omega)\right\}$$

$$+ 12\bar{F}_{29,29,13}\left\{\bar{C}_{29}^{-1,3}\sin(\Phi + \omega) - \bar{S}_{29}^{-1,3}\cos(\Phi + \omega)\right\}$$

$$\left. + \text{terms in } e^{|q|-1}\left\{q - \tfrac{1}{2}(k + q)e^2\right\}\begin{matrix}\cos\\ \sin\end{matrix}(\gamma\Phi - q\omega)\right] \quad . \tag{12}$$

This time, 16 sets of values of i or e were fitted by integrated forms of (11) or (12), as described in section 7.1 (for 14th-order), between December 1973 and April 1974. Fig 8 shows the variations of Φ and $\dot{\Phi}$: exact 29:2 resonance ($\dot{\Phi} = 0$) occurred on 2 March 1974 (MJD 42108). Only three PROP values were available, combined with 13 US Navy values (with standard deviations as for 14th-order resonance).

As for 14th-order resonance, $(\gamma, q) = (1, 0)$ gave the best least-squares fit for i alone, shown in Fig 9a. However, for e alone, the best fit, given in Fig 9b, was obtained with $(\gamma, q) = (1, \pm 1)$, where $[q, k] = [1, 1]$ and $[-1, 3]$. A simultaneous least-squares fit to i and e was made using the SIMRES program[18] for $(\gamma, q) = (1, 0), (1, \pm 1)$. The resulting sets of lumped values for the 29th-order harmonic coefficients are:

(1) Inclination i alone:

$$10^9\bar{C}_{29}^{0,2} = 50 \pm 20 \ , \qquad 10^9\bar{S}_{29}^{0,2} = -\ 160 \pm 70 \ , \tag{13}$$

where $\varepsilon = 0.63$.

(2) Eccentricity e alone:

$$\left.\begin{aligned} 10^9\bar{C}_{29}^{1,1} &= 40 \pm 610 \ , & 10^9\bar{S}_{29}^{1,1} &= -\ 2750 \pm 860 \ , \\ 10^9\bar{C}_{29}^{-1,3} &= -\ 980 \pm 590 \ , & 10^9\bar{S}_{29}^{-1,3} &= -\ 1950 \pm 700 \ , \end{aligned}\right\} \tag{14}$$

where $\varepsilon = 0.72$.

(3) For i and e simultaneously:

$$\left.\begin{aligned} 10^9\bar{C}_{29}^{0,2} &= 340 \pm 230 \ , & 10^9\bar{S}_{29}^{0,2} &= -\ 360 \pm 200 \\ 10^9\bar{C}_{29}^{1,1} &= -\ 240 \pm 280 \ , & 10^9\bar{S}_{29}^{1,1} &= -\ 510 \pm 340 \\ 10^9\bar{C}_{29}^{-1,3} &= -\ 620 \pm 300 \ , & 10^9\bar{S}_{29}^{-1,3} &= -\ 260 \pm 250 \ , \end{aligned}\right\} \tag{15}$$

with a weighting factor of 1.41 and $\varepsilon = 0.61$. The values in (14) and (15) cannot be regarded as reliable because the standard deviations are so large, but the values (13) are better and may be useful in future in deriving individual coefficients of 29th order.

It is to be expected that the numerical values of the lumped coefficients would be poor because the total variations in i and e are no greater than the errors in the observational values. However, Fig 9 is valuable in showing that the overall changes in both i and e are virtually zero in passing through 29:2 resonance, due to the effects of resonance itself, and the fitting at resonance provided the end points for the Λ curves in Fig 1. After restoring the atmospheric-rotation perturbation, the inclination variation was mapped into the appropriate gap in Fig 1.

7.3 15th order

The 15th-order resonance equations[18,20], ignoring e^2 terms, may be
107 expressed as:

$$\frac{di}{dt} = \frac{n}{\sin i}\left(\frac{R}{a}\right)^{15}\Bigg[(15 - \cos i)\bar{F}_{15,15,7}\left\{\bar{C}^{0,1}_{15} \sin \Phi - \bar{S}^{0,1}_{15} \cos \Phi\right\}$$
$$+ \left(\frac{R}{a}\right)\frac{17e}{2}\bar{F}_{16,15,8}(15)\left\{\bar{S}^{1,0}_{15} \sin(\Phi - \omega) + \bar{C}^{1,0}_{15} \cos(\Phi - \omega)\right\}$$
$$+ \left(\frac{R}{a}\right)\frac{13e}{2}(15 - 2 \cos i)\bar{F}_{16,15,7}\left\{\bar{S}^{-1,2}_{15} \sin(\Phi + \omega) + \bar{C}^{-1,2}_{15} \cos(\Phi + \omega)\right\}\Bigg] \quad (16)$$

and the corresponding terms in the equation for e are:

$$\frac{de}{dt} = n\left(\frac{R}{a}\right)^{15}\Bigg[\frac{e}{2}\bar{F}_{15,15,7}\left(\bar{C}^{0,1}_{15} \sin \Phi - \bar{S}^{0,1}_{15} \cos \Phi\right)$$
$$- \left(\frac{R}{a}\right)\frac{17}{2}\bar{F}_{16,15,8}\left\{\bar{S}^{1,0}_{15} \sin(\Phi - \omega) + \bar{C}^{1,0}_{15} \cos(\Phi - \omega)\right\}$$
$$+ \left(\frac{R}{a}\right)\frac{13}{2}\bar{F}_{16,15,7}\left\{\bar{S}^{-1,2}_{15} \sin(\Phi + \omega) + \bar{C}^{-1,2}_{15} \cos(\Phi + \omega)\right\}\Bigg] \ . \quad (17)$$

15th-order resonance has been investigated between 4 December 1974 and 13 June 1975, where 13 PROP orbits were available (Table 1) as well as 10 US Navy orbits. Exact 15th-order resonance ($\dot{\Phi} = 0$) occurred on 9 March 1975: Fig 10 shows the variations of Φ and $\dot{\Phi}$.

The best least-squares fitting of the integrated form of equation (16) to the 23 values of perturbation-free inclination was given by $(\gamma, q) = (1, 0)$. The lumped values for 15th-order odd harmonic coefficients are:-

$$10^9\bar{C}^{0,1}_{15} = -37 \pm 6 \ , \qquad 10^9\bar{S}^{0,1}_{15} = 10 \pm 6 \ , \quad (18)$$

with $\varepsilon = 0.58$. Fig 11 shows the inclination values and the fitted curve. The fitting is entirely satisfactory and the change in inclination should be large enough to give reliable values of the lumped coefficients. Fig 11 also clearly shows an increase of 0.004° in inclination due to 15th-order resonance.

Various fittings were attempted with eccentricity values, using equation (17), but no satisfactory results were obtained and so no graph is shown.

7.4 31:2 resonance

No reliable values of lumped 31st-order geopotential harmonic coefficients 107
can be expected here, as resonance passed rather rapidly. However, a least-squares fitting was made for $(\gamma, q) = (1, 0)$ in order to determine the overall

change in inclination. The resonance region considered was between 14 October and 25 December 1975 and Fig 12 shows the variations of Φ and $\dot{\Phi}$. Exact resonance, where $\dot{\Phi} = 0$, occurred on 19 November. Ten PROP and nine US Navy inclination values were fitted by a least-squares curve after removing the usual perturbations, to give 31st-order lumped coefficients as:

$$10^9 \bar{C}^{0,2}_{31} = 24 \pm 18 , \quad 10^9 \bar{S}^{0,2}_{31} = 30 \pm 23 , \tag{20}$$

with $\varepsilon = 0.99$. The fitting is quite satisfactory, and the coefficients are as good as can be expected when drag is so high.

Atmospheric rotation has a strong influence at this late stage in the satellite's life and Fig 13a shows the values of inclination originally and after removal of the perturbation due to an atmosphere rotating at $\Lambda = 1.05$ rev/day. It can be seen that this perturbation can change the inclination by up to 0.01°. Fig 13b gives the inclination values with the perturbation removed, showing the best least-squares fitting. The overall change in i due to resonance, in passing through the resonance, is virtually zero and so can be ignored in Fig 1.

8 CONCLUSIONS

The orbit of China 2 rocket, 1971-18B, has been determined at 114 epochs between 1971 and 1976, using more than 7000 radar and optical observations, including 170 observations made by Hewitt cameras. The standard deviations in inclination varied from 0.0003 to 0.0026°, and the sd in eccentricity was between 3×10^{-6} (equivalent to 22 m in perigee height) and 44×10^{-6}.

Values of density scale height have been determined from the change in perigee height and compared with values calculated from the *CIRA 1972* reference atmosphere: the agreement is good between April 1971 and October 1975, but the ensuing observational values (near decay) are about 10 per cent lower, on average.

Four values of atmospheric rotation rate Λ have been determined for heights y between 270 and 315 km. All four give west-to-east winds (super-rotation). The results (Fig 1) are:

(1) $\Lambda = 1.15 \pm 0.05$ at $y = 315$ km between April 1971 and August 1972;

(2) $\Lambda = 1.05 \pm 0.05$ at $y = 310$ km between December 1972 and December 1973;

(3) $\Lambda = 1.10 \pm 0.05$ at $y = 295$ km between April 1974 and January 1975;

107 (4) $\Lambda = 1.05 \pm 0.05$ at $y = 270$ km between May 1975 and February 1976.

The values (1), (3) and (4) are for mean (evening and morning) conditions; the value (2) has a slight morning bias.

The effects of four orbital resonances, of order 14:1, 29:2, 15:1 and 31:2, have been investigated, and the lumped harmonic coefficients in the geopotential have been determined. Although not of great accuracy, these values should be of use, in combination with values from satellites at other inclinations, in determining individual harmonic coefficients. The analyses of the resonances were necessary to determine the overall change in inclination and eccentricity on passing resonance, and they served this purpose well. However, the difficulties encountered suggest that accurate values of harmonic coefficients for the 29:2 and 31:2 resonances cannot be obtained from a high-drag satellite unless a number of very accurate orbits from Hewitt camera observations are available close to the time of resonance.

Further orbits were determined for each day during the final 15 days before decay in February 1976 from 1400 NORAD observations: the accuracy of these daily orbits was very consistent, and slightly better than the average of the original 114 orbits. Analysis of the change in inclination in the last 12 days before decay revealed a very strong west-to-east wind, of 240 ± 40 m/s, at a mean height of 195 km, at a local time of 19-23 h and at a latitude of 15-50° N in winter (5-16 February 1976). This is the highest reliable wind speed obtained from analysis of satellite orbits: it arises because the satellite's perigee was at the evening maximum of the zonal wind, and because of the fine time resolution and excellent accuracy of the daily orbits. Analysis of the perigee height gave a further 10 values of density scale height H with a sharper time resolution than has previously been possible, and an accuracy of about ±3 per cent. These values of H, like those in the preceding three months, are about 10 per cent lower than indicated by *CIRA 1972*.

Table 1

ORBITAL PARAMETERS FOR CHINA 2 ROCKET, WITH STANDARD DEVIATIONS

Orbit	MJD	Date	a	e	i	Ω	ω	M_0	M_1	M_2	M_3	M_4	M_5	ε	D	N
1	41068	1971 Apr 27	7403.9249 7	0.102908 15	69.9039 14	169.196 2	124.898 10	279.280 9	4906.8071 7	0.1516 5	−0.00156 8	0.00015 4	-	0.64	7.7	62
2	076	May 5	7401.6121 9	0.102578 14	69.9006 11	152.597 2	114.993 12	303.023 10	4909.1075 9	0.1379 5	0.00062 9	0.00032 3	-	0.68	8.4	41
3*	096	May 25	7395.5575 3	0.101997 5	69.9005 6	111.023 1	90.308 7	265.754 6	4915.1386 3	0.1185 1	−0.00065 3	-	-	0.71	9.0	45
4*	105	Jun 3	7393.2521 8	0.101730 7	69.9023 7	92.282 1	79.132 6	231.596 5	4917.4384 8	0.1592 2	0.00006 6	−0.00041 1	-	0.54	8.8	38
5	137	Jul 5	7382.7167 13	0.100327 17	69.9018 17	25.472 1	39.443 7	72.745 7	4927.9705 13	0.1534 2	−0.0032 1	-	-	0.66	8.0	40
6	145	Jul 13	7380.7358 8	0.099986 19	69.8995 19	8.717 2	29.469 8	264.917 8	4929.9549 8	0.1094 2	0.00021 5	-	-	0.62	9.9	35
7	180	Aug 17	7373.2557 7	0.098516 14	69.9043 12	295.272 1	345.605 5	149.246 6	4937.4607 7	0.0919 4	0.00083 4	0.00008 2	-	0.50	9.4	57
8*	189	Aug 26	7371.2001 9	0.098145 13	69.9008 10	276.345 1	334.267 5	315.058 6	4939.5265 10	0.1320 1	0.00060 7	-	-	0.48	7.9	70
9*	197	Sep 3	7369.0098 7	0.097793 14	69.8986 8	259.505 1	324.174 6	240.070 6	4941.7293 7	0.1263 5	−0.0020 1	0.00012	-	0.51	6.8	83
10	204	Sep 10	7367.1547 10	0.097508 14	69.8984 10	244.754 1	315.313 8	278.618 9	4943.5964 10	0.1263 9	−0.0018 2	0.00029 9	-	0.52	6.1	69
11*	212	Sep 18	7364.9801 10	0.097177 7	69.8981 3	227.881 1	305.231 3	235.839 4	4945.7864 10	0.1585 7	0.0069 5	0.0009 1	-	0.64	6.1	79
12*	220	Sep 26	7362.3797 7	0.096781 7	69.9010 6	210.992 1	295.037 8	212.894 9	4948.4078 7	0.1746 6	0.00009 6	−0.00077 3	-	0.53	9.0	62
13*	229	Oct 5	7359.9665 13	0.096500 3	69.9039 8	191.973 2	283.568 10	120.407 11	4950.8424 13	0.1151 6	−0.0011 2	-	-	0.61	6.5	71
14*	232	Oct 8	7359.3034 25	0.096345 10	69.9023 10	185.631 2	279.732 11	213.996 13	4951.5116 25	0.1119 29	0.0119 41	-	-	0.48	2.0	56
15*	235	Oct 11	7358.6202 10	0.096282 7	69.9019 7	179.286 1	275.905 10	309.638 11	4952.2013 11	0.1022 8	−0.0017 1	0.00077 7	-	0.49	6.5	60
16*	240	Oct 16	7357.5530 16	0.096111 10	69.9031 9	168.704 1	269.537 11	233.389 12	4953.2791 16	0.0921 12	−0.0048 7	0.0007 2	-	0.54	5.7	60
17*	246	Oct 22	7356.5665 18	0.096017 11	69.9005 10	156.003 2	261.894 6	76.125 7	4954.2756 19	0.0836 29	0.0020 6	0.0012 6	-	0.56	4.1	55
18	252	Oct 28	7355.4360 14	0.095923 7	69.8985 10	143.293 1	254.239 5	285.343 5	4955.4180 14	0.1032 6	0.0083 3	0.00035 4	−0.00025 1	0.45	8.4	52
19	270	Nov 15	7350.4727 7	0.095459 8	69.8990 9	105.114 1	231.311 5	245.480 6	4960.4392 7	0.1604 3	0.00020 6	0.00021 2	-	0.42	9.3	48
20	281	Nov 26	7346.2436 11	0.095100 7	69.9007 11	81.739 1	217.283 5	112.297 6	4964.7244 11	0.2229 3	−0.0020 1	−0.00038 2	-	0.46	8.9	47
21	294	Dec 9	7340.7119 8	0.094651 8	69.9029 10	54.058 1	200.723 5	250.467 5	4970.3387 8	0.2128 5	0.0027 1	−0.00003 3	−0.000048 7	0.47	9.4	45
22	306	Dec 21	7335.5136 21	0.094166 22	69.8986 17	28.444 2	185.381 8	166.352 8	4975.6241 21	0.1983 7	−0.0021 3	0.00036 3	−0.00003 1	0.77	9.4	37
23	329	1972 Jan 13	7328.4579 11	0.093664 20	69.8946 17	339.222 2	156.032 9	214.076 8	4982.8130 12	0.1407 2	−0.00044 8	-	-	0.69	9.0	43
24	340	Jan 24	7325.0952 15	0.093440 14	69.8956 15	315.633 1	142.021 8	323.039 8	4986.2455 15	0.1818 5	−0.0009 2	−0.00034 3	0.000055 6	0.54	10.1	37
25	351	Feb 4	7321.4994 13	0.093062 19	69.8940 16	292.010 1	127.939 15	112.535 13	4989.9201 13	0.1555 4	−0.0022 2	-	-	0.74	5.9	28

Table 1 (continued)

Orbit	MJD	Date	a	e	i	Ω	ω	M_0	M_1	M_2	M_3	M_4	M_5	ε	D	N
26	41361	1972 Feb 14	7318.5070	0.092809	69.8949	270.504	115.235	346.581	4992.9816	0.1755	0.0012	-0.00018	0.000039	0.66	9.9	56
			8	7	7	1	8	7	8	4	1	2	5			
27	391	Mar 15	7306.4464	0.091380	69.8911	205.754	76.769	206.949	5005.3522	0.1879	0.0054	0.00012	-0.000097	0.71	9.4	39
			12	10	11	1	13	11	13	5	2	2	8			
28*	422	Apr 15	7294.2885	0.089656	69.8897	138.516	36.881	41.082	5017.8743	0.2731	0.00206	-0.00014	-	0.74	9.3	43
			9	9	6	1	7	6	9	3	6	2				
29*	433	Apr 26	7288.2153	0.088834	69.8886	114.550	22.654	192.506	5024.1491	0.2698	0.00140	0.00037	-	0.45	10.6	43
			7	15	9	1	6	7	7	4	5	1				
30*	445	May 8	7281.7835	0.087846	69.8902	88.336	7.056	43.179	5030.8087	0.2687	0.00356	0.00030	-	0.28	7.1	43
			4	9	4	1	3	3	4	4	4	3				
31*	450	May 13	7278.9615	0.087425	69.8901	77.394	0.535	4.413	5033.7353	0.3027	0.00166	-	-	0.53	4.9	41
			18	24	9	2	9	9	19	7	36					
32*	456	May 19	7275.3874	0.086929	69.8927	64.240	352.685	338.155	5037.4461	0.2693	-0.00425	-	-	0.59	4.9	33
			17	14	8	1	7	9	18	3	32					
33	481	Jun 13	7266.1517	0.085419	69.8898	9.262	319.790	43.979	5047.0555	0.1375	-0.00141	0.00030	-	0.60	9.9	55
			7	14	11	1	8	8	8	4	4	2				
34*	516	Jul 18	7258.7068	0.084178	69.8932	292.003	273.350	80.634	5054.8242	0.0971	0.00023	-0.00014	-	0.50	9.5	54
			5	8	5	1	9	10	5	5	4	2				
35	529	Jul 31	7255.9683	0.083859	69.8916	263.249	256.024	291.238	5057.6867	0.1092	0.00077	0.00037	-	0.43	8.2	62
			9	8	10	1	9	10	10	5	8	3				
36	540	Aug 11	7252.9148	0.083570	69.8854	238.881	241.371	143.204	5060.8815	0.1161	-0.0073	0.0008	-	0.48	5.3	50
			11	10	9	1	7	8	12	15	2	2				
37	547	Aug 18	7251.6709	0.083485	69.8838	223.363	232.047	294.125	5062.1840	0.0968	0.0053	-	-	0.33	5.0	41
			11	11	11	1	8	8	12	6	3					
38	554	Aug 25	7249.9816	0.083410	69.8844	207.833	222.706	95.524	5063.9539	0.1355	0.0055	0.0011	-	0.41	5.9	40
			14	13	13	1	8	8	15	13	2	1				
39	561	Sep 1	7247.4379	0.083207	69.8878	192.290	213.424	272.087	5066.6210	0.2055	0.0012	-	-	0.37	4.1	34
			12	13	12	1	7	8	13	17	6					
40	574	Sep 14	7242.7158	0.082760	69.8882	163.382	196.133	291.631	5071.5781	0.1861	0.0025	-	-	0.84	7.0	51
			14	24	18	2	11	11	15	5	2					
41	582	Sep 22	7240.1223	0.082621	69.8891	145.561	185.542	195.584	5074.3041	0.1622	0.0047	0.00083	-	0.66	7.7	43
			14	23	15	2	9	9	14	8	2	6				
42*	665	Dec 14	7204.3373	0.078991	69.8753	318.796	74.915	191.224	5112.1670	0.1513	0.00423	-0.00005	-	0.41	9.6	32
			4	6	6	1	9	8	4	1	3	1				
43*	698	1973 Jan 16	7192.1928	0.077191	69.8750	243.843	30.615	259.314	5125.1240	0.1639	-0.0049	0.00022	-	0.81	7.5	44
			11	13	8	1	8	9	11	9	1	7				
44	706	Jan 24	7189.6570	0.076838	69.8706	225.606	19.831	230.467	5127.8360	0.1730	-0.0014	0.00053	-	0.57	8.9	28
			14	20	17	2	10	10	15	7	1	4				
45*	727	Feb 14	7182.7159	0.075588	69.8720	177.632	351.345	353.805	5135.2727	0.1683	0.00054	0.00025	-	0.49	9.7	41
			5	16	5	1	6	6	5	4	3	2				
46	741	Feb 28	7177.6835	0.074729	69.8743	145.562	332.203	284.470	5140.6757	0.1796	-0.0008	0.00016	-0.000034	0.43	9.6	52
			13	12	10	1	7	8	14	5	2	2	7			
47*	757	Mar 16	7172.5672	0.073887	69.8709	108.820	310.227	138.977	5146.1782	0.1830	0.00090	-	-	0.52	9.7	80
			4	10	4	1	8	9	5	2	4					
48*	764	Mar 23	7169.7492	0.073504	69.8692	92.717	300.561	172.487	5149.2132	0.2169	-0.0049	-	-	0.69	2.1	73
			12	26	6	1	12	15	13	17	16					
49*	768	Mar 27	7168.3791	0.073245	69.8680	83.506	295.013	252.512	5150.6898	0.1628	-0.00041	0.0008	-	0.37	5.9	53
			10	12	5	1	11	13	11	8	16	1				
50*	775	Apr 3	7165.8266	0.072925	69.8699	67.369	285.312	316.275	5153.4429	0.2270	-0.0101	-0.00121	0.00027	0.50	8.9	73
			16	10	8	1	12	14	17	5	3	3	1			

07

Table 1 (continued)

Orbit	MJD	Date	a	e	i	Ω	ω	M_0	M_1	M_2	M_3	M_4	M_5	ε	D	N
51	41789	1973 Apr 17	7161.4938	0.072348	69.8735	35.050	265.877	138.065	5158.1218	0.1428	-0.0024	0.00017	-	0.50	7.9	47
			10	10	13	1	14	16	11	8	1	5				
52	798	Apr 26	7159.4807	0.072123	69.8763	14.247	253.399	131.340	5160.2982	0.1296	0.00135	-0.00017	-	0.52	8.6	44
			10	11	11	1	13	14	11	5	8	3				
53*	847	Jun 14	7143.9945	0.070910	69.8723	260.556	185.452	276.486	5177.0906	0.2237	-0.00117	-0.00012	-	0.53	9.7	48
			9	18	9	1	8	9	10	3	7	2				
54*	857	Jun 24	7139.8580	0.070486	69.8708	237.246	171.618	229.815	5181.5914	0.2369	0.0093	-0.0011	-0.00018	0.61	7.3	45
			16	16	8	1	10	10	17	18	4	3	5			
55*	867	Jul 4	7136.1398	0.070319	69.8644	213.891	157.824	227.418	5185.6423	0.1363	-0.00478	0.00052	-	0.47	9.5	49
			5	13	10	1	7	7	6	4	4	2				
56*	902	Aug 8	7128.2351	0.069620	69.8697	131.949	109.442	71.256	5194.2731	0.1364	0.00123	-0.00035	-0.000033	0.51	9.6	42
			9	3	5	1	9	8	10	2	14	1	5			
57*	972	Oct 17	7105.6723	0.066293	69.8654	326.930	12.201	177.632	5219.0389	0.2069	0.0098	-0.00005	-0.00015	0.71	9.5	42
			15	11	7	1	9	9	16	4	2	2	1			
58*	993	Nov 7	7094.8762	0.064643	69.8611	277.027	342.573	97.267	5230.9588	0.2682	-0.00271	-0.00009	-	0.46	9.9	38
			6	14	6	1	8	8	6	3	4	1				
59*	42004	Nov 18	7090.3162	0.063872	69.8625	250.789	326.904	66.501	5236.0073	0.2377	0.0039	-	-	0.89	4.9	38
			8	11	10	1	12	11	8	6	2					
60	020	Dec 4	7084.1030	0.062896	69.8613	212.526	303.987	21.520	5242.8989	0.1706	0.0016	-0.00008	-0.00011	0.60	8.7	72
			11	9	10	1	7	8	12	8	2	5	1			
61	028	Dec 12	7082.1265	0.062571	69.8621	193.358	292.485	214.506	5245.0944	0.1017	-0.0028	0.00038	-	0.49	7.9	67
			9	8	10	1	8	9	11	4	2	4				
62	064	1974 Jan 17	7072.8926	0.061444	69.8673	106.893	240.633	207.048	5255.3723	0.2186	0.0014	-0.00026	-	0.45	9.4	41
			13	8	9	1	9	8	14	5	1	2				
63*	076	Jan 29	7068.5678	0.061076	69.8631	77.975	223.313	301.469	5260.1972	0.1617	-0.0032	0.00069	-0.000062	0.63	9.1	69
			7	6	4	1	11	12	8	6	1	4	7			
64	091	Feb 13	7064.5193	0.060784	69.8594	41.754	201.693	38.171	5264.7206	0.1778	-0.0006	-0.00067	-	0.53	9.4	60
			6	16	11	1	9	10	7	5	1	2				
65*	181	May 14	7026.7305	0.056870	69.8549	182.422	72.340	120.591	5307.2583	0.2027	0.0029	0.0014	0.00012	0.68	6.6	35
			14	7	10	1	21	19	16	9	5	1	4			
66*	185	May 18	7025.0333	0.056606	69.8567	172.582	66.573	113.275	5309.1823	0.2306	-0.0081	-	-	0.69	2.8	44
			13	6	5	1	12	11	15	14	11					
67*	210	Jun 12	7013.9480	0.054987	69.8552	110.880	30.454	143.866	5321.7769	0.3487	-0.0017	-0.00093	0.00009	0.62	9.6	32
			23	24	12	2	18	17	27	4	4	2	1			
68*	220	Jun 22	7008.7949	0.054124	69.8599	86.105	15.778	112.571	5327.6490	0.2440	-0.0073	-	-	0.62	4.9	38
			15	17	11	2	5	7	17	3	3					
69	278	Aug 19	6990.2930	0.050736	69.8560	301.447	289.469	226.761	5348.8201	0.1638	0.0082	-0.00014	-0.00012	0.68	9.6	52
			14	13	12	2	23	24	16	6	2	3	1			
70	289	Aug 30	6987.1839	0.050338	69.8519	273.889	272.919	44.779	5352.3914	0.1574	0.00129	-0.00012	-	0.49	9.8	79
			5	9	10	1	18	19	6	4	4	2				
71	300	Sep 10	6984.1411	0.050027	69.8491	246.283	256.287	260.928	5355.8904	0.1475	-0.00047	-	-	0.53	8.3	68
			9	10	10	1	18	19	11	1	8					
72	315	Sep 25	6979.1325	0.049504	69.8523	208.571	233.614	1.669	5361.6587	0.1825	0.0032	0.00028	-0.00009	0.62	9.5	48
			18	15	18	2	20	22	21	8	3	3	1			
73	329	Oct 9	6973.6422	0.049000	69.8529	173.291	212.609	226.330	5367.9936	0.3050	0.0066	-0.00011	-	0.80	9.6	35
			9	23	15	2	22	23	11	11	1	4				
74	364	Nov 13	6949.3004	0.046596	69.8439	84.472	159.955	290.541	5396.2298	0.4897	-0.0028	-0.00093	-0.00012	0.72	9.0	33
			18	22	15	2	18	18	21	10	4	4	1			
75	385	Dec 4	6936.5215	0.045218	69.8455	30.676	128.177	22.512	5411.1529	0.2656	-0.0081	-0.00083	0.00014	0.71	9.0	34
			19	13	17	2	18	18	23	7	4	3	1			

Table 1 (continued)

Orbit	MJD	Date	a	e	i	Ω	ω	M_0	M_1	M_2	M_3	M_4	M_5	ε	D	N
76	42413	1975 Jan 1	6926.5787	0.044081	69.8444	318.559	86.148	138.688	5422.8115	0.1880	-0.0014	0.00047	0.000073	0.46	9.5	32
			7	6	9	1	17	16	8	4	1	1	5			
77	437	Jan 25	6916.5660	0.042591	69.8426	256.453	50.137	105.392	5434.5943	0.2100	-0.0019	-0.00004	-	0.85	10.8	54
			9	11	11	1	13	14	10	3	1	1				
78	449	Feb 6	6911.9235	0.041929	69.8416	225.283	31.836	192.120	5440.0720	0.2379	0.00099	0.00031	-	0.62	10.1	44
			4	6	8	1	10	10	5	4	3	1				
79	498	Mar 27	6889.9236	0.038112	69.8427	97.179	315.722	265.214	5466.1558	0.2985	0.0055	-0.00028	-0.00007	0.63	9.9	43
			13	16	13	1	23	24	16	8	2	5	1			
80	510	Apr 8	6884.1121	0.037250	69.8401	65.587	296.605	21.922	5473.0808	0.3222	0.0095	-0.00043	-0.00020	0.58	9.8	37
			17	13	17	1	29	31	20	5	3	2	1			
81	523	Apr 21	6878.8483	0.036481	69.8458	31.268	275.784	300.031	5479.3662	0.1869	0.0014	-0.00064	-	0.48	9.0	58
			10	9	13	1	26	27	12	5	1	3				
82*	533	May 1	6876.3922	0.036184	69.8456	4.825	259.772	30.096	5482.3030	0.1366	0.0064	-0.00061	-0.00004	0.54	8.6	68
			10	11	8	1	30	32	12	7	3	4	1			
83	542	May 10	6873.5381	0.035899	69.8446	340.994	245.410	66.077	5485.7189	0.1766	-0.0028	-	-	0.54	8.2	55
			11	15	16	2	35	37	13	4	1					
84	550	May 18	6871.1651	0.035677	69.8410	319.781	232.744	42.691	5488.5616	0.2033	-0.0029	0.00048	0.00034	0.40	7.2	57
			12	11	11	1	15	16	14	7	6	7	4			
85	558	May 26	6868.0726	0.035376	69.8384	298.535	219.968	45.875	5492.2698	0.2627	0.0062	-0.00039	-0.00011	0.52	8.7	57
			25	17	13	1	23	24	30	9	5	7	2			
86	568	Jun 5	6863.3892	0.035011	69.8421	271.936	204.169	275.766	5497.8944	0.3184	-0.0026	-0.00076	-	0.45	8.0	58
			10	15	11	1	18	19	12	6	1	4				
87	576	Jun 13	6859.6454	0.034726	69.8426	250.609	191.532	356.977	5502.3973	0.3286	0.0025	-0.00196	-0.00017	0.51	7.9	46
			16	22	13	1	19	20	20	11	4	10	2			
88	585	Jun 22	6855.1892	0.034275	69.8391	226.571	177.365	223.342	5507.7647	0.2649	-0.0033	-0.00024	-	0.47	8.0	56
			8	19	12	1	15	16	10	6	1	4				
89	592	Jun 29	6852.3611	0.034053	69.8340	207.841	166.367	269.700	5511.1755	0.2485	0.0104	0.0012	-0.00039	0.50	8.0	50
			18	10	9	1	11	12	22	14	4	2	3			
90	603	Jul 10	6847.4964	0.033637	69.8328	178.347	148.903	84.319	5517.0511	0.3339	-0.0114	-0.00192	0.00033	0.68	8.5	37
			39	22	20	2	27	26	47	8	7	5	3			
91	615	Jul 22	6842.3234	0.033146	69.8358	146.094	130.260	86.755	5523.3110	0.2276	-0.0033	0.00073	0.00012	0.57	9.1	52
			12	14	9	1	27	25	15	5	2	3	1			
92*	623	Jul 30	6838.8524	0.032730	69.8388	124.551	117.756	9.490	5527.5178	0.2311	-0.0018	0.00154	-	0.50	6.6	32
			8	6	9	1	28	27	10	6	2	6				
93	631	Aug 7	6834.9051	0.032278	69.8364	102.963	105.338	326.777	5532.3082	0.3544	-0.0029	0.00039	0.00029	0.62	7.5	33
			23	13	14	2	44	42	28	9	6	6	4			
94	641	Aug 17	6828.1936	0.031479	69.8349	75.910	89.632	248.898	5540.4692	0.4061	-0.0156	-0.00037	0.00035	0.55	9.2	26
			21	12	19	2	45	43	25	7	4	4	2			
95	651	Aug 27	6822.3357	0.030692	69.8312	48.764	73.878	249.622	5547.6084	0.3446	0.00508	0.00073	-	0.55	9.9	32
			6	13	13	1	37	36	7	7	4	3				
96	663	Sep 8	6814.5967	0.029617	69.8359	16.085	55.029	276.628	5557.0644	0.4703	0.0020	-0.00096	0.00051	0.54	7.0	28
			36	12	17	1	37	36	44	8	9	9	5			
97	670	Sep 15	6809.2461	0.028881	69.8354	356.955	43.935	319.945	5563.6175	0.3584	-0.0067	0.00117	-	0.49	7.9	33
			12	17	14	2	29	28	15	5	2	5				
98	679	Sep 24	6803.8560	0.027960	69.8337	332.300	29.726	21.496	5570.2319	0.3652	-0.0027	0.00095	0.00030	0.50	7.6	47
			17	17	12	1	26	25	21	8	5	5	3			
99	687	Oct 2	6797.8403	0.027093	69.8315	310.317	16.808	331.415	5577.6296	0.4820	0.0035	0.00143	0.00015	0.47	7.9	57
			13	8	9	1	17	17	16	5	4	4	2			
100*	699	Oct 14	6785.5796	0.025278	69.8252	277.185	357.600	29.300	5592.7576	0.6680	0.0063	-0.00015	-0.00011	0.43	8.0	67
			9	14	7	1	17	17	11	5	3	3	2			
101	707	Oct 22	6776.6029	0.023950	69.8278	254.973	344.387	175.779	5603.8775	0.6908	-0.0022	-0.00031	-	0.48	7.9	62
			7	18	9	1	22	24	9	6	1	4				

107

Table 1 (concluded)

Orbit	MJD	Date	a	e	i	Ω	ω	M_0	M_1	M_2	M_3	M_4	M_5	ε	D	N
102	42715	1975 Oct 30	6768.1576	0.022706	69.8264	232.668	331.077	49.068	5614.3727	0.6920	0.00045	-0.00139	-	0.53	7.6	62
			8	12	11	1	23	23	10	7	8	4				
103	723	Nov 7	6758.9860	0.021399	69.8286	210.268	317.157	10.222	5625.8078	0.5868	-0.0220	0.0033	0.00070	0.54	7.1	45
			25	18	15	2	53	55	31	13	9	1	6			
104	731	Nov 15	6751.1880	0.020312	69.8252	187.761	303.390	56.994	5635.5604	0.5041	-0.0071	0.00197	0.00030	0.57	7.2	48
			21	17	15	2	53	54	26	11	10	9	7			
105*	739	Nov 23	6743.7770	0.019365	69.8225	165.166	289.380	177.900	5644.8553	0.6885	0.0042	-0.0052	-0.00041	0.67	7.3	56
			22	11	8	1	42	42	28	15	9	1	6			
106	747	Dec 1	6736.9873	0.018533	69.8197	142.485	275.454	12.524	5653.3935	0.6310	0.0111	-0.00307	-	0.50	7.6	58
			10	11	12	2	67	69	13	8	1	6				
107	755	Dec 9	6729.4549	0.017636	69.8194	119.720	261.679	278.457	5662.8909	0.6628	0.0160	-0.00169	-0.00041	0.59	7.7	64
			23	12	13	2	65	68	29	10	6	6	3			
108	763	Dec 17	6721.0092	0.016740	69.8206	96.862	248.096	263.898	5673.5717	0.7441	-0.0049	-0.00259	0.00027	0.46	7.1	61
			21	10	12	1	62	64	27	9	7	7	4			
109	771	Dec 25	6712.2880	0.015743	69.8228	73.912	234.561	336.686	5684.6363	0.7724	0.0404	0.00285	-0.00086	0.50	7.5	56
			19	11	12	1	42	42	24	8	6	5	3			
110	778	1976 Jan 1	6702.0751	0.014723	69.8201	53.721	222.489	215.247	5697.6387	0.8126	-0.0174	0.00208	0.00044	0.60	6.8	48
			19	13	13	1	49	51	25	15	7	15	6			
111	786	Jan 9	6691.1186	0.013519	69.8167	30.533	208.417	131.043	5711.6431	0.8505	-0.0051	0.0072	0.0011	0.53	5.2	40
			27	22	16	2	68	69	35	29	21	7	3			
112	798	Jan 21	6670.6838	0.011435	69.8160	355.435	187.598	68.742	5737.9168	1.1515	0.0222	0.00240	-0.00035	0.76	8.8	34
			46	33	18	2	76	79	60	9	8	6	3			
113	812	Feb 4	6638.4948	0.008400	69.8110	313.965	161.588	24.201	5779.7137	2.0322	0.0161	0.00246	-	0.47	7.2	24
			9	44	20	2	126	125	12	10	2	8				
114	820	Feb 12	6599.7955	0.005271	69.8014	289.869	146.240	352.358	5830.6397	4.7950	0.2546	0.08067	0.0057	0.64	4.0	18
			49	41	26	4	335	332	65	95	50	40	16			

Key:
- MJD Modified Julian Day
- a semi major axis (km)
- e eccentricity
- i inclination (deg)
- Ω right ascension of node (deg)
- ω argument of perigee (deg)
- * orbits with Hewitt camera observations
- M_0 mean anomaly at epoch (deg)
- M_1 mean motion, n (deg/day)
- M_2-M_5 additional coefficients in polynomial for M
- ε measure of fit
- D time coverage of observations (days)
- N number of observations used

Table 3

ORBITAL PARAMETERS FOR THE FINAL 15 DAYS BEFORE DECAY

Orbit	MJD	Date	a	e	i	Ω	ω	M_0	M_1	M_2	ε	D	N
A	42810.0	1976 Feb 2	6644.603	0.009014	69.8127	319.9555	165.17	352.76	5771.744	1.99	0.89	0.88	99
			3	17	11	15	7	7	4	2			
B	11.0	Feb 3	6641.597	0.008791	69,8136	316.9723	163.30	6.56	5775.664	2.06	0.63	0.96	93
			2	11	7	7	4	4	2	1			
C	12.0	Feb 4	6638.494	0.008536	69.8118	313.9894	161.50	24.30	5779.715	2.01	0.64	0.89	83
			2	12	10	10	5	5	3	1			
D	13.0	Feb 5	6635.322	0.008208	69.8133	310.9916	159.74	46.04	5783.861	2.23	0.60	0.89	80
			3	11	10	10	5	5	3	1			
E	14.0	Feb 6	6632.051	0.007925	69.8126	307.9947	157.83	72.18	5788.142	2.25	0.59	0.69	79
			4	9	9	8	5	5	5	2			
F	15.0	Feb 7	6628.653	0.007731	69.8108	304.9943	156.27	102.33	5792.594	2.29	0.82	1.36	77
			1	16	9	12	7	7	2	1			
G	16.0	Feb 8	6624.508	0.007283	69.8110	301.9843	154.32	137.55	5798.034	3.41	0.70	0.74	83
			3	8	7	6	5	5	4	1			
H	17.0	Feb 9	6618.978	0.006825	69.8089	298.9691	152.26	179.37	5805.304	3.93	0.83	0.77	89
			2	9	8	8	6	6	3	1			
I	18.0	Feb 10	6613.099	0.006331	69.8068	295.9435	150.15	228.80	5813.049	4.11	0.66	1.00	82
			2	8	7	8	6	6	2	1			
J	19.0	Feb 11	6606.671	0.005841	69,8041	292.9097	147.96	286.43	5821.537	4.40	0.65	0.93	78
			2	9	8	10	9	9	2	1			
K	20.0	Feb 12	6599.745	0.005268	69.8028	289.8660	145.66	352.94	5830.707	4.81	0.64	0.93	72
			2	8	9	10	9	9	3	1			
L	21.0	Feb 13	6591.639	0.004680	69.7996	286.8060	143.10	69.48	5841.469	6.16	0.60	0.80	66
			3	8	8	9	11	11	3	1			
M	22.0	Feb 14	6580.692	0.003940	69.7966	283.7306	139.29	159.69	5856.055	8.88	0.98	0.81	78
			3	10	11	12	21	21	4	2			
N	23.0	Feb 15	6564.396	0.003048	69.7925	280.6310	136.08	267.03	5877.881	13.25	0.66	0.53	60
			6	7	9	6	16	16	8	3			
P	24.0	Feb 16	6522.207	0.001380	69.7831	277.4893	125.94	53.43	5935.024	79.94**	1.00	0.56	79
			17	9	11	12	39	39	23	25			

See Table 1 for key.

$$**\begin{cases} M_3 = 90.1 \pm 1.0 \\ M_4 = 56.7 \pm 1.3 \end{cases}$$

REFERENCES

No.	Author	Title, etc
1	R.H. Gooding R.J. Tayler	A PROP 3 users' manual. RAE Technical Report 68299 (1968)
2	C.J. Brookes F.C. Ryland	Air density at heights near 300 km, from analysis of the orbit of China 2 rocket (1971-18B). *Planet.Space Sci.*, 25, 1011-1020 (1977)
3	D.W. Scott	ORES: a computer program for analysis of residuals from PROP. RAE Technical Report 69163 (1969)
4	G.E. Cook	Basic theory for PROD, a program for computing the development of satellite orbits. *Celestial Mechanics*, 7, 301-314 (1973) RAE Technical Report 71007 (1971)
5	D.G. King-Hele D.M.C. Walker	Air density at heights near 150 km in 1970, from the orbit of Cosmos 316 (1969-108A). *Planet. Space Sci.*, 19, 1637-51 (1971) RAE Technical Report 71129 (1971)
6	D.G. King-Hele	*Theory of satellite orbits in an atmosphere.* Butterworths, London (1964)
7	-	*CIRA 1972* (Cospar International Reference Atmosphere 1972). Akademie-Verlag, Berlin (1972)
8	L.G. Jacchia	Revised static models of the thermosphere and exosphere with empirical temperature profiles. Smithsonian Astrophys. Obs. Spec. Rpt. 332 (1971)
9	D.M.C. Walker	Variations in air density from January 1972 to April 1975 at heights near 200 km. *Planet. Space Sci.*, 26, 291-309 (1978) RAE Technical Report 77078 (1977)
10	D.G. King-Hele D.W. Scott	A revaluation of the rotational speed of the upper atmosphere. *Planet. Space Sci.*, 14, 1339-1365 (1966) RAE Technical Report 66189 (1966)

7

107

REFERENCES (continued)

No.	Author	Title, etc
11	D.G. King-Hele D.M.C. Walker	Upper-atmosphere zonal winds: variation with height and local time. *Planet. Space Sci.*, 25, 313-336 (1977) RAE Technical Report 76055 (1976)
12	R.G. Roble J.E. Salah B.A. Emery	The seasonal variation of the diurnal thermospheric winds over Millstone Hill during solar cycle maximum. *Journ. Atmos. Terr. Phys.*, 39, 503-511 (1977)
13	D.G. King-Hele	The effect of a meridional wind on a satellite orbit. *Proc. Roy. Soc.* A, 294, 261-272 (1966) RAE Technical Report 66010 (1966)
14	B.K. Ching J.M. Straus	Ionospheric model effects on thermospheric calculations. *Journ. Atmos. Terr. Phys.*, 39, 1389-1394 (1977)
15	D.G. King-Hele D.M.C. Walker R.H. Gooding	Evaluation of 14th-order harmonics in the geopotential. RAE Technical Report 78015 (1978)
16	R.R. Allan	Resonant effect on inclination for close satellites. *Planet. Space Sci.*, 21, 205-225 (1973) RAE Technical Report 71245 (1971)
17	R.H. Gooding	Lumped geopotential coefficients $\bar{C}_{15,15}$ and $\bar{S}_{15,15}$ obtained from resonant variation in the orbit of Ariel 3. RAE Technical Report 71068 (1971)
18	R.H. Gooding	Studies of resonance in the orbits of Ariel satellites. RAE Technical Report (to be issued)
19	D.M.C. Walker	29th-order harmonics in the geopotential from the orbit of Ariel 1 at 29:2 resonance. *Planet. Space Sci.*, 25, 337-342 (1977) RAE Technical Report 76110 (1976)
20	J. Klokočník	Changes in the inclination of a close earth satellite due to orbital resonances. *Bull. Astronom. Inst. Czechoslovakia*, 27, 287-295 (1976)

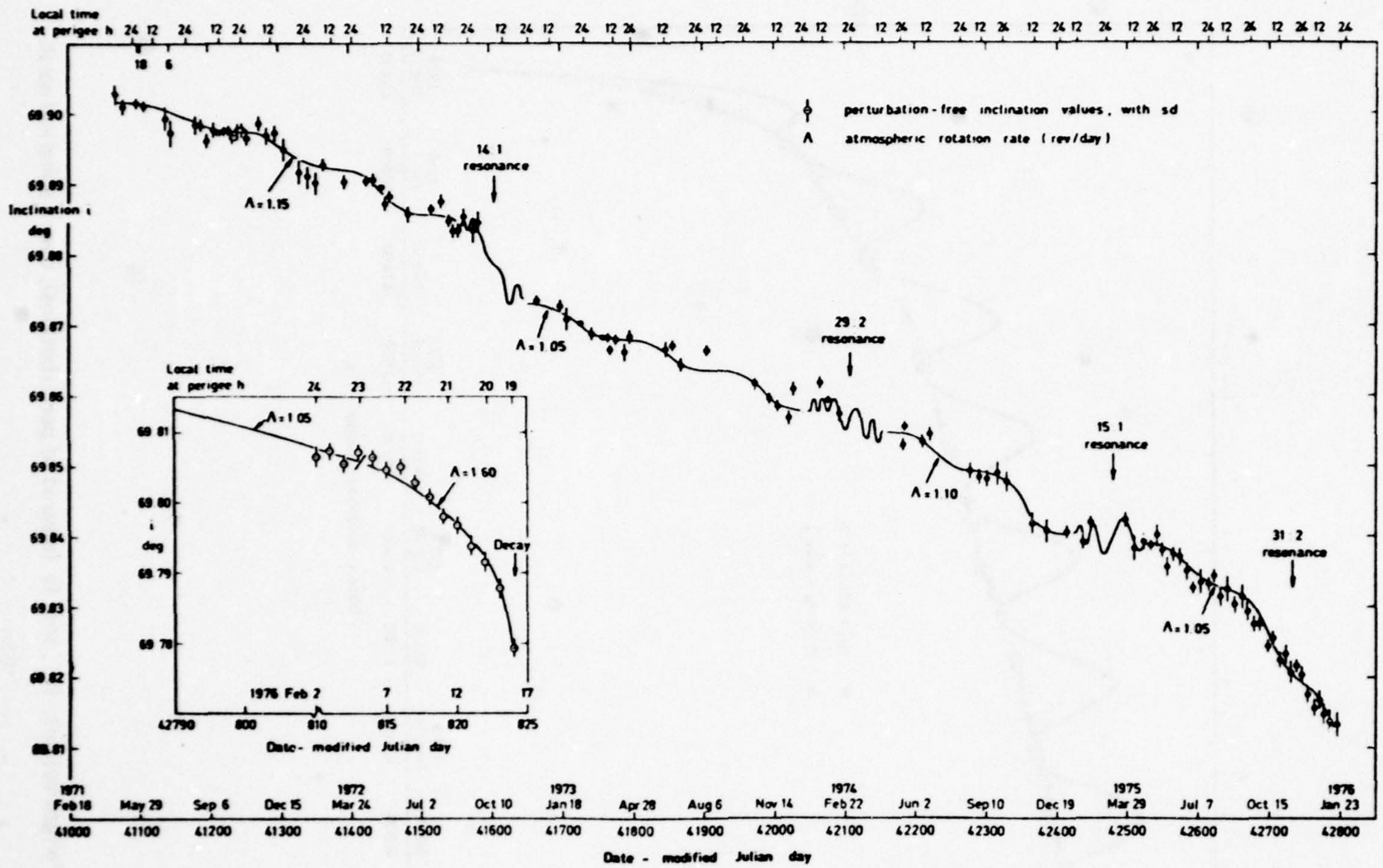

Fig 1 Perturbation-free inclination for China 2 rocket, showing fitted Λ-curves

Fig 2

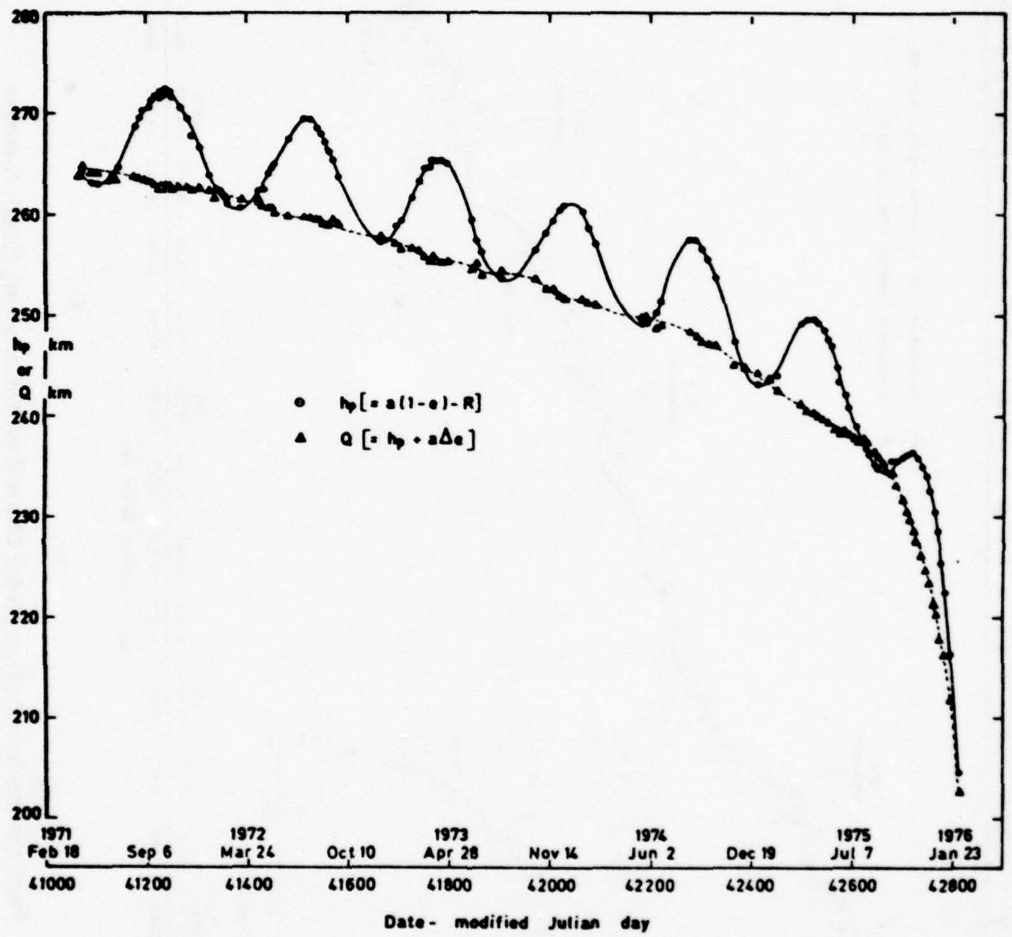

Fig 2 Perigee heights, h_p, and Q (cleared of perturbations), over a spherical earth

TR 78107

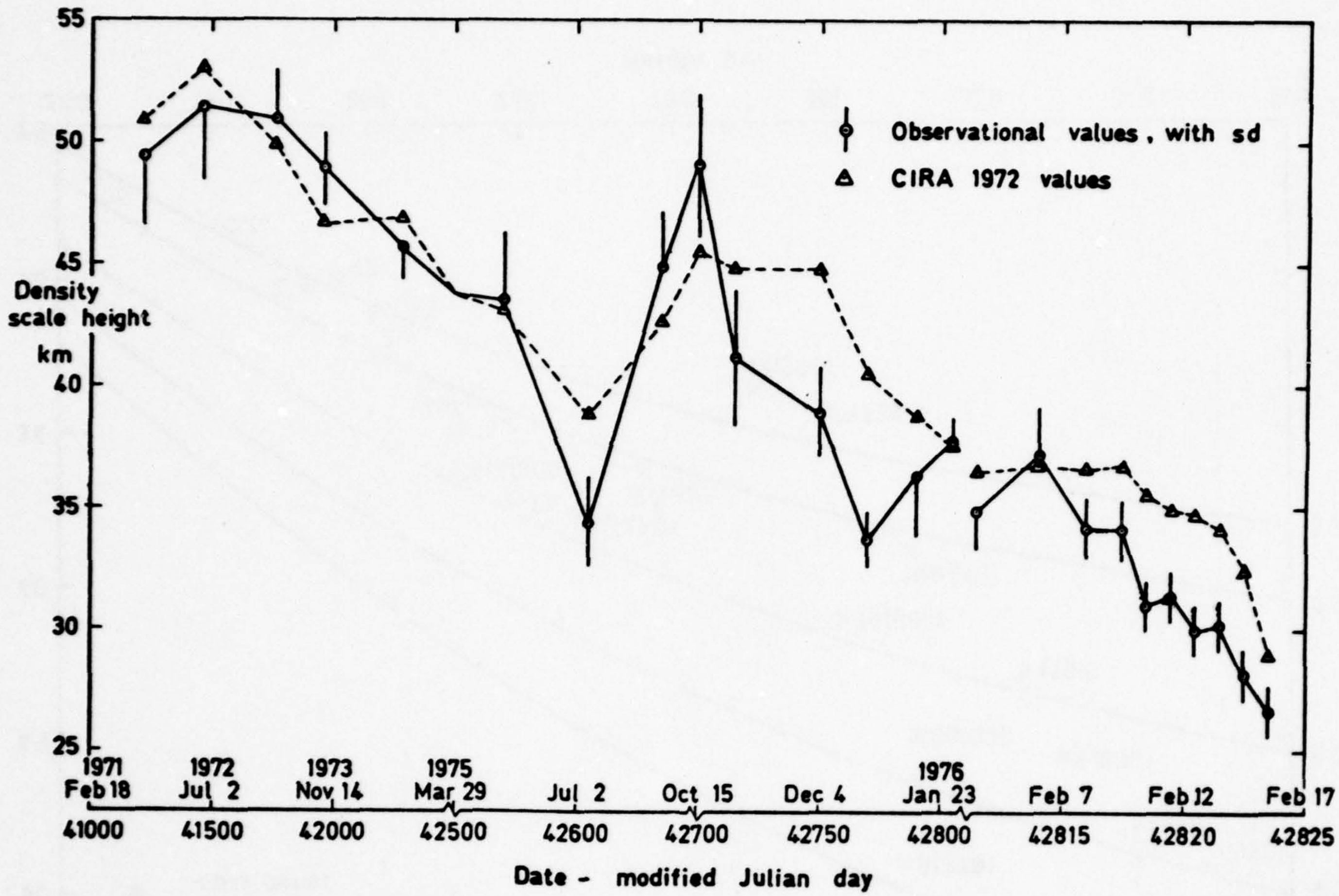

Fig 3 Density scale height compared with CIRA 1972 values

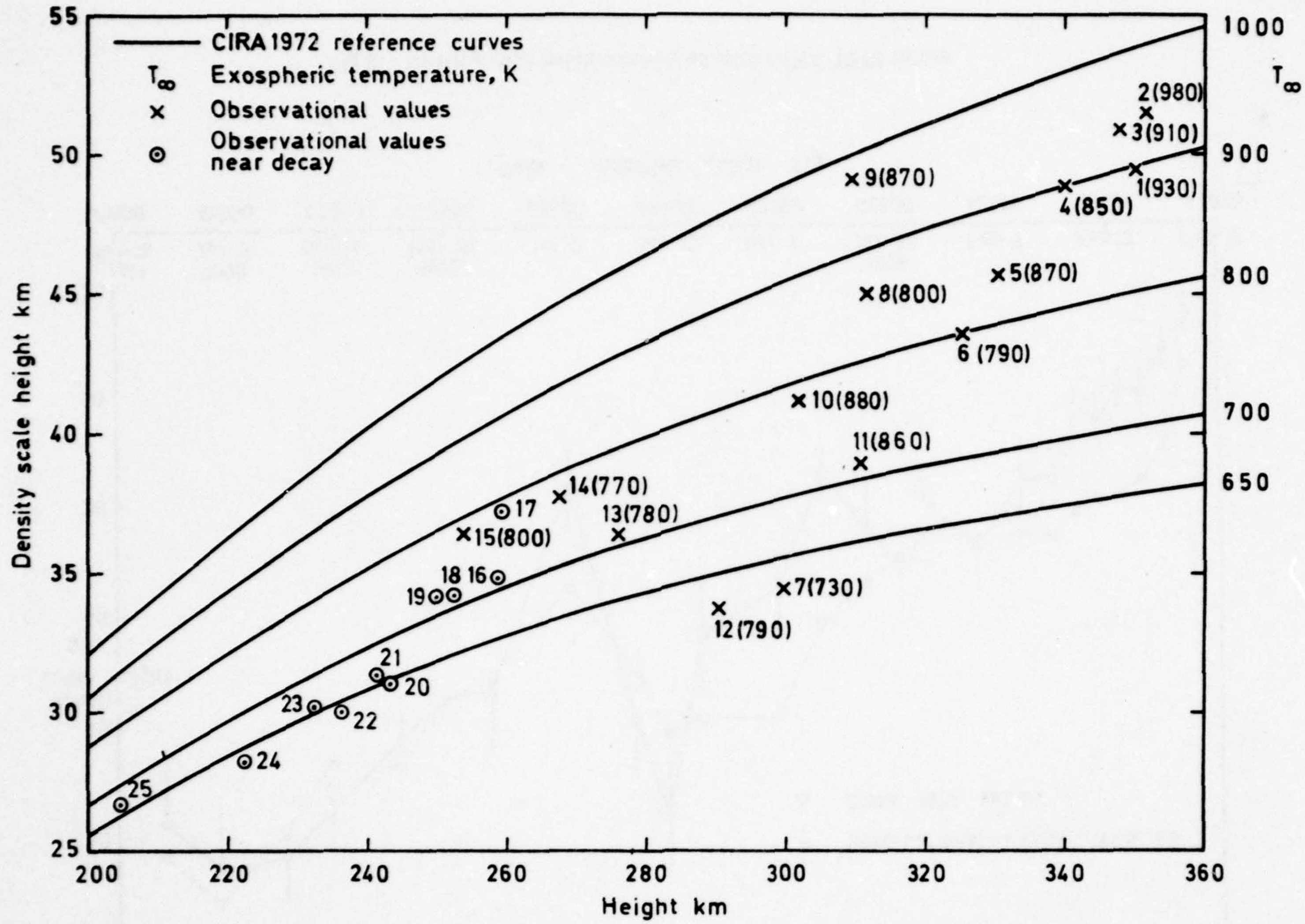

Fig 4 Density scale height values compared with CIRA 1972 curves

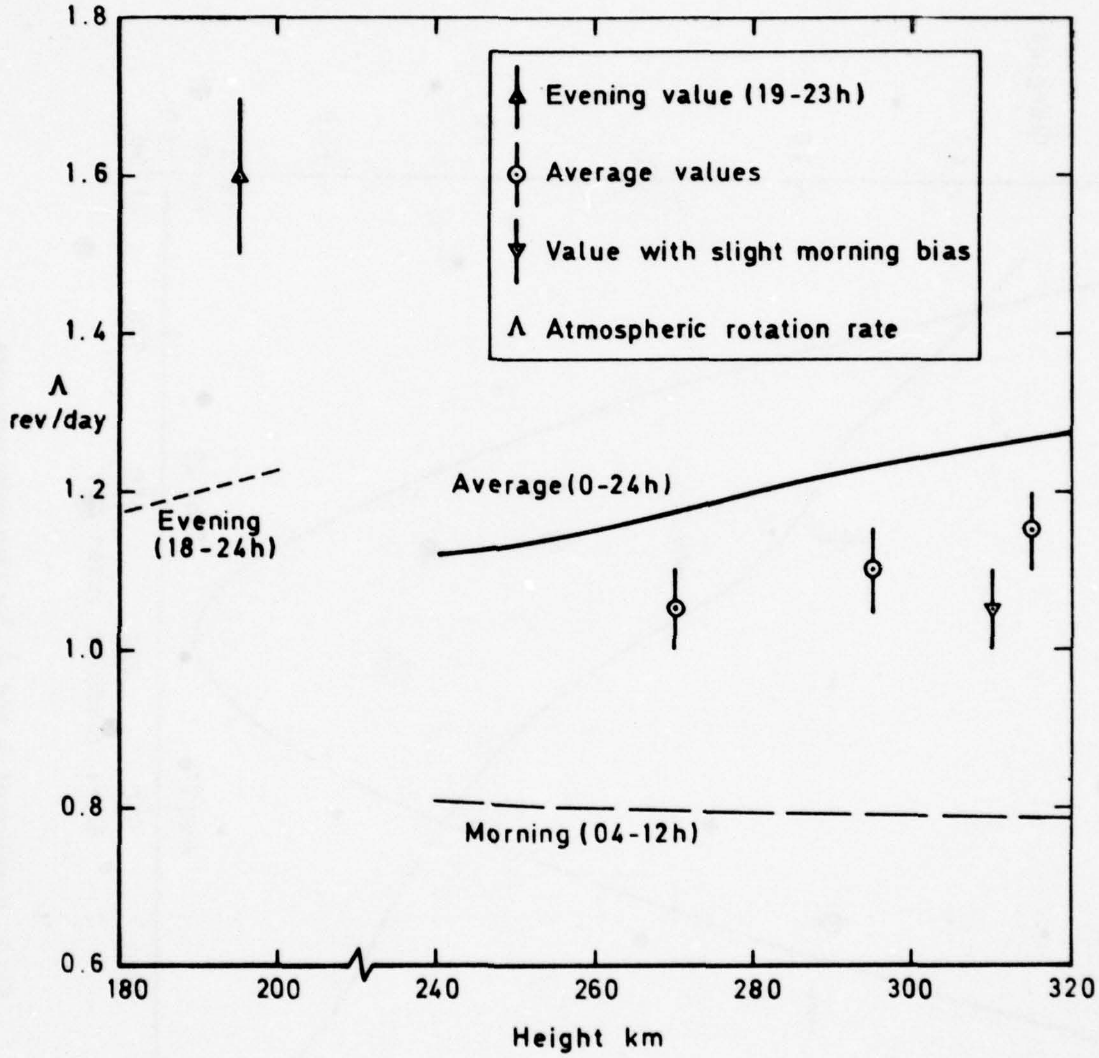

Fig 5 Values of Λ obtained from the orbit of 1971-18B, with curves from Ref 11

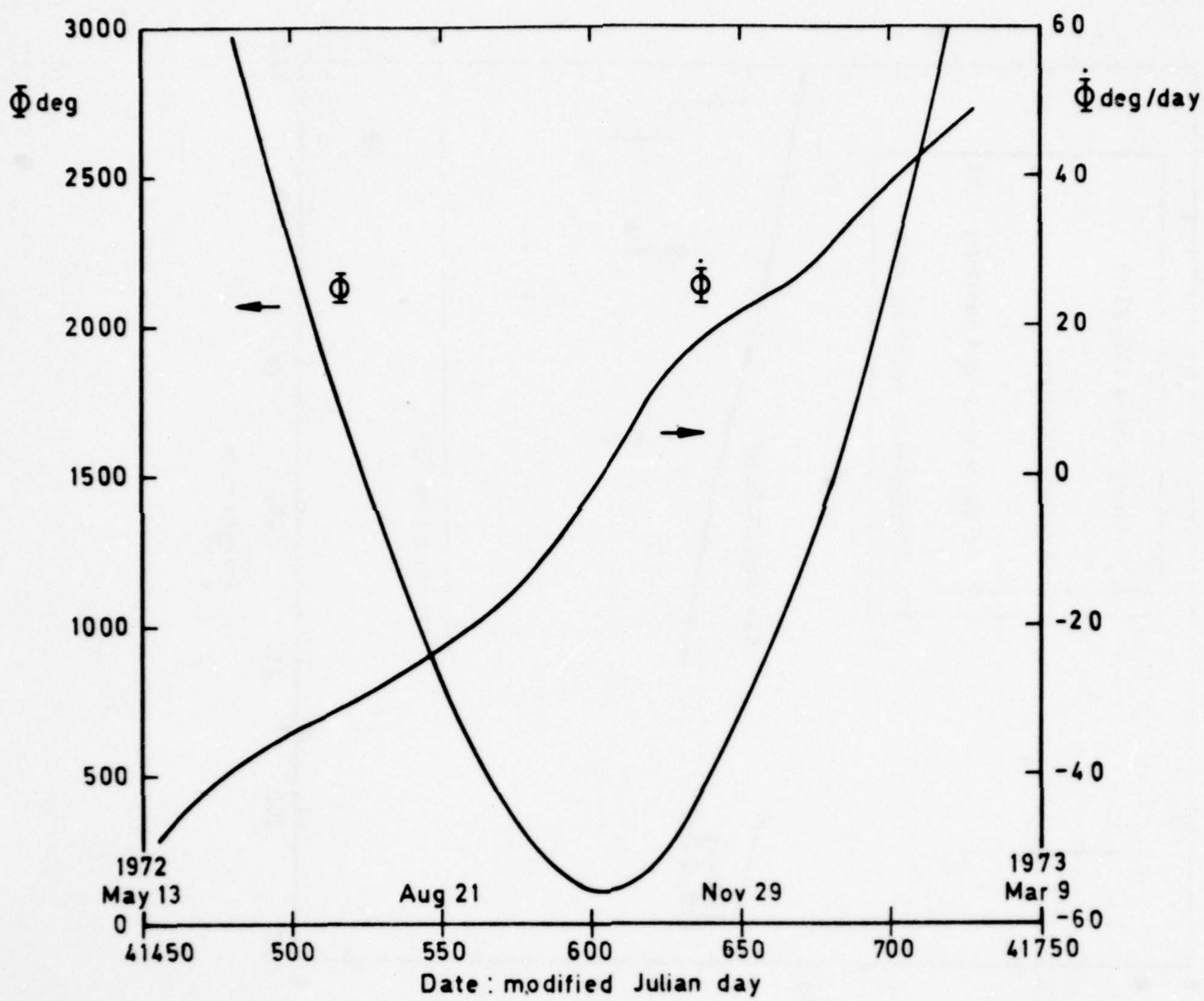

Fig 6 Variation of Φ and $\dot{\Phi}$, for 14th-order resonance

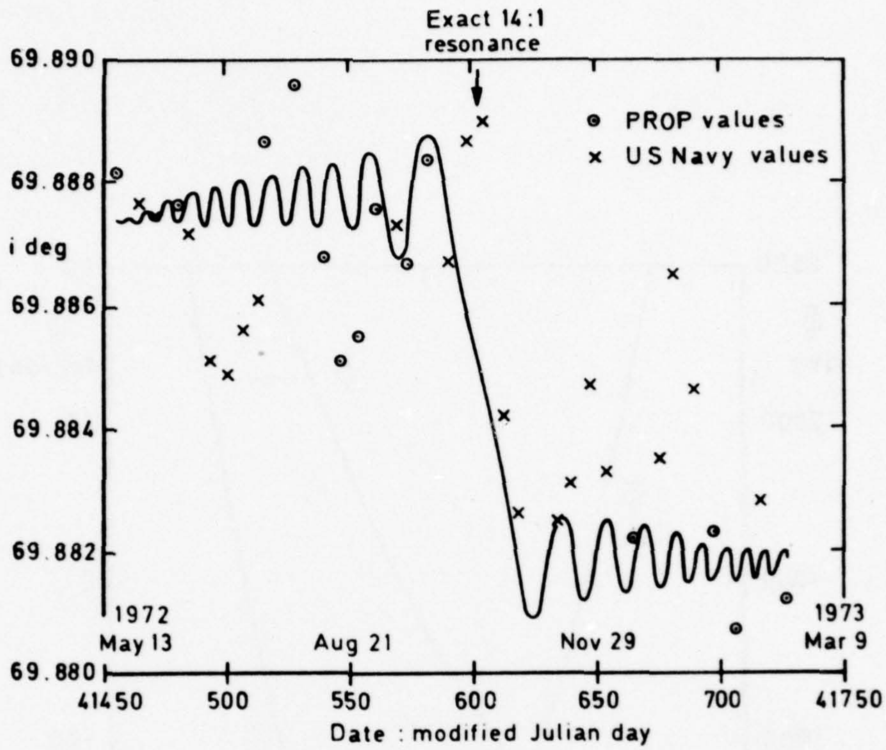

a Inclination

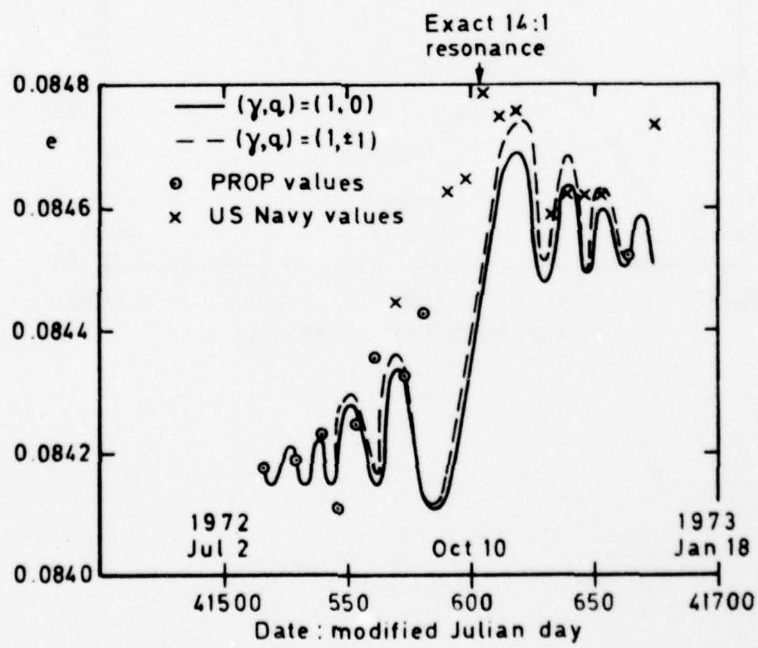

b Eccentricity

Fig 7a&b Values for 14th-order resonance, with fitted curves

Fig 8

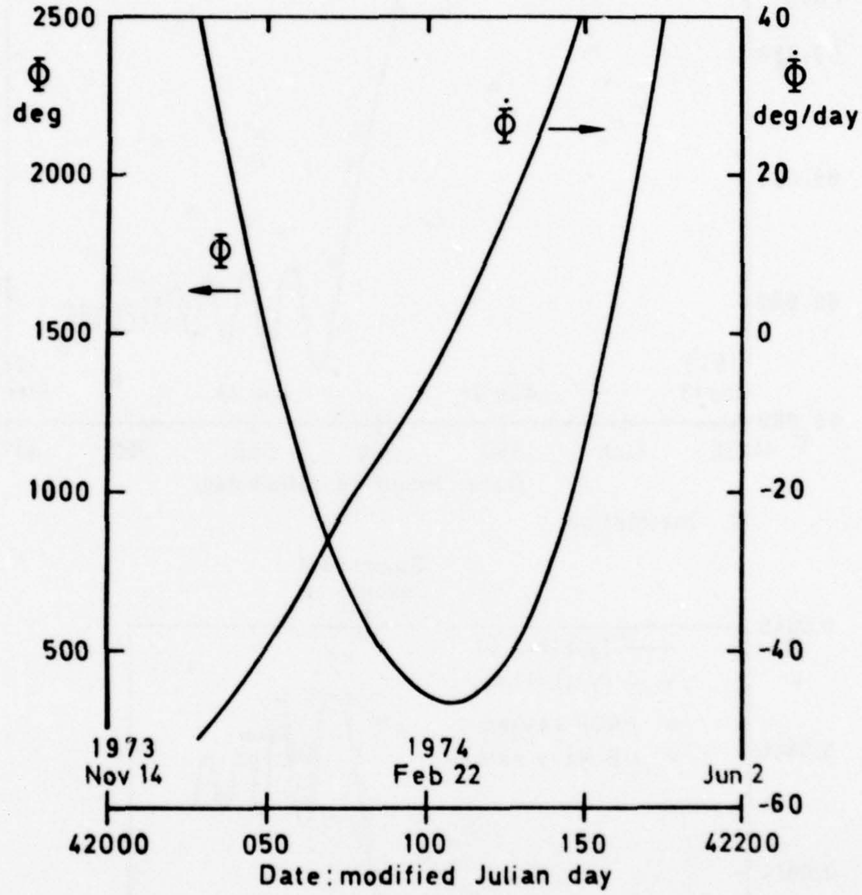

Fig 8 Φ and $\dot{\Phi}$, for 29:2 resonance

TR 78107

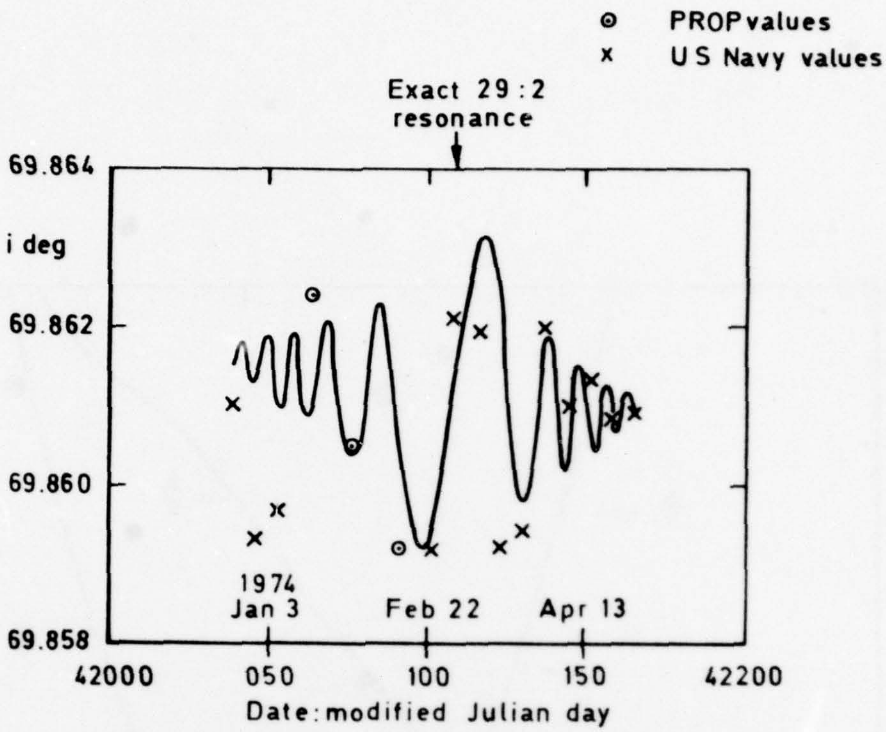

a Inclination

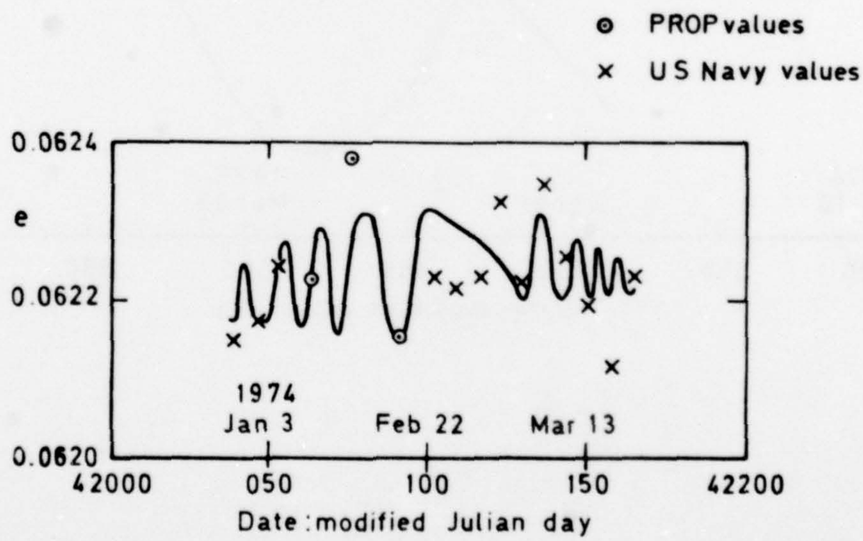

b Eccentricity

Fig 9a&b Values for 29:2 resonance, with fitted curves

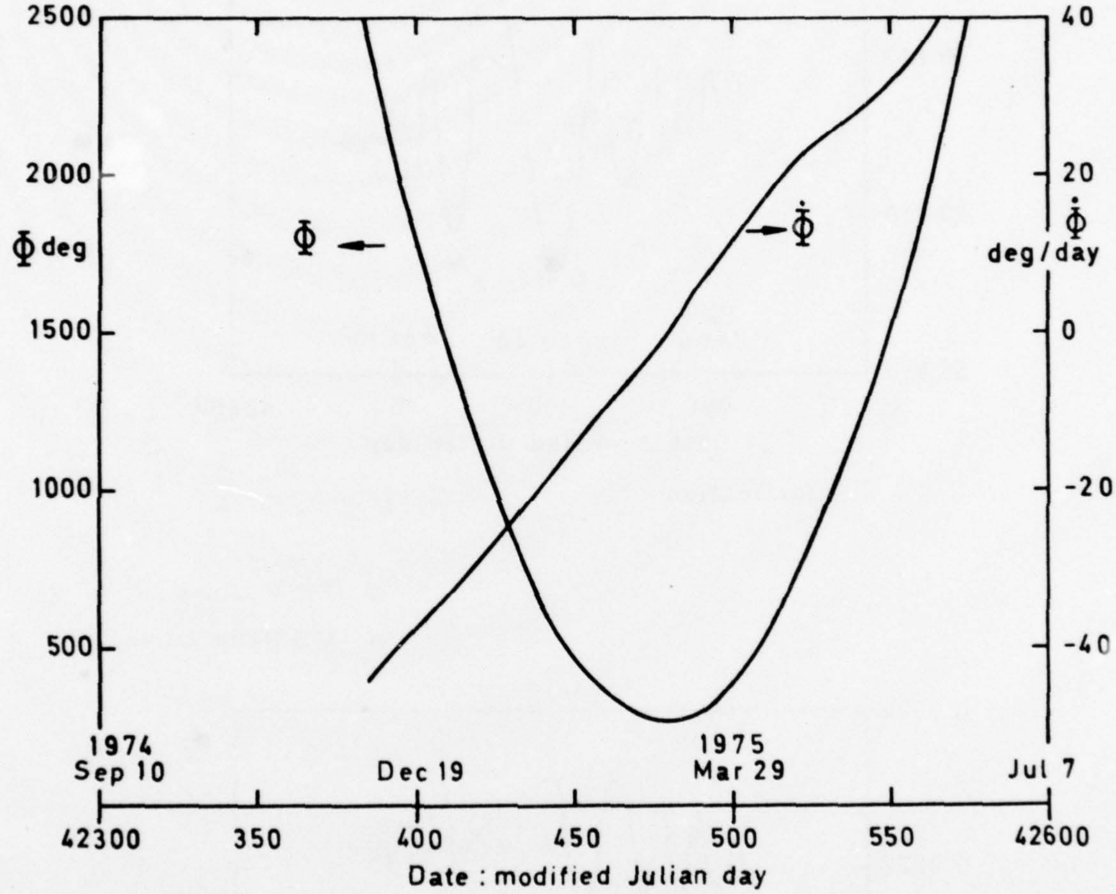

Fig 10 Φ and $\dot{\Phi}$, for 15th-order resonance

TR 78107

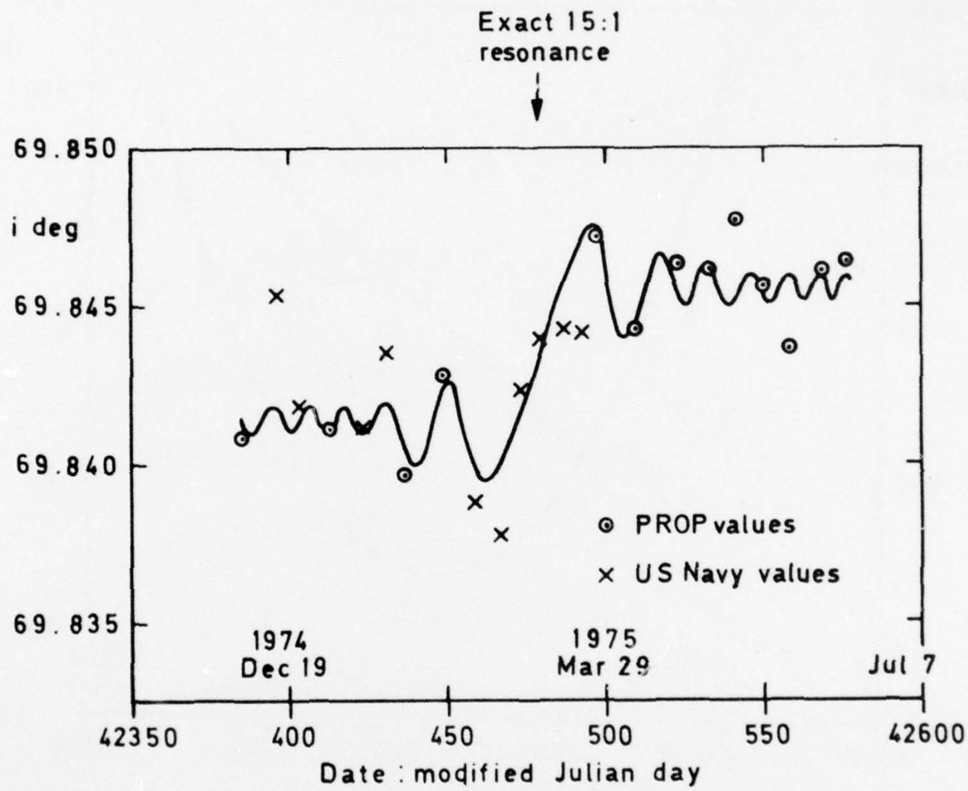

Fig 11 Inclination values for 15th-order resonance, with fitted curve

Fig 12

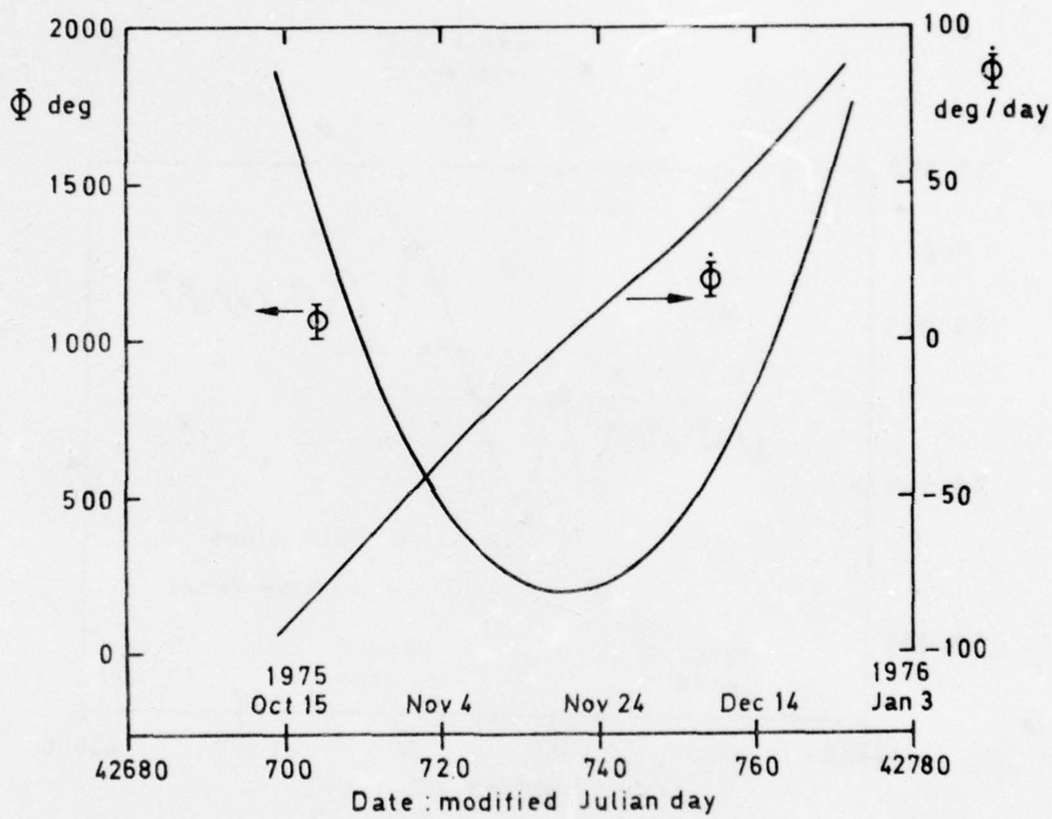

Fig 12 Φ and $\dot{\Phi}$, for 31:2 resonance

TR 78107

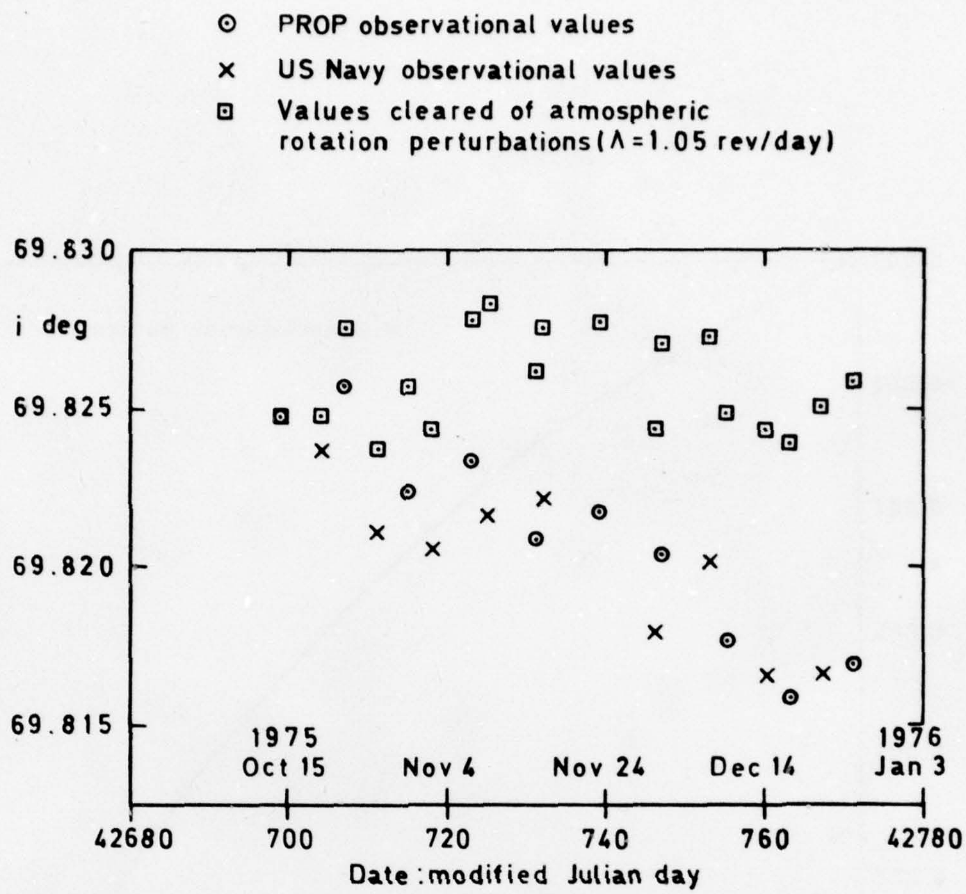

a The removal of atmospheric-rotation perturbations

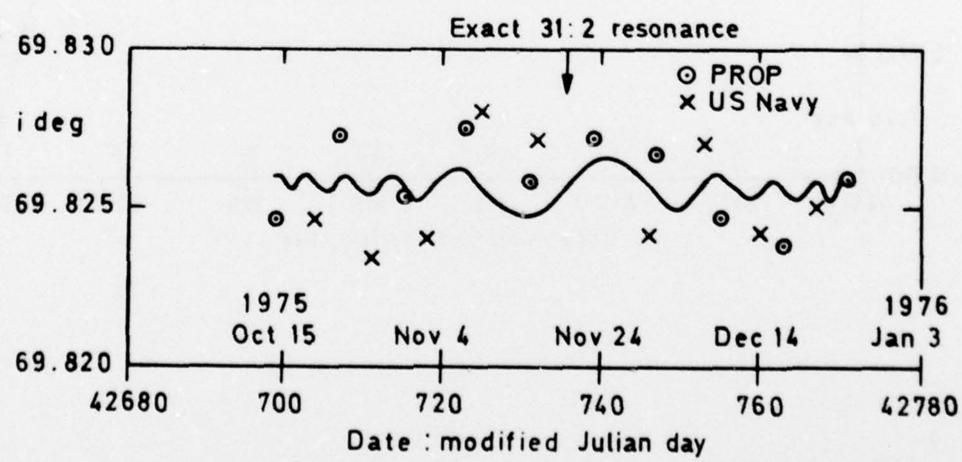

b Fitting of curve to perturbation - free values

TR 78107

Fig 13a&b Values of inclination for 31:2 resonance

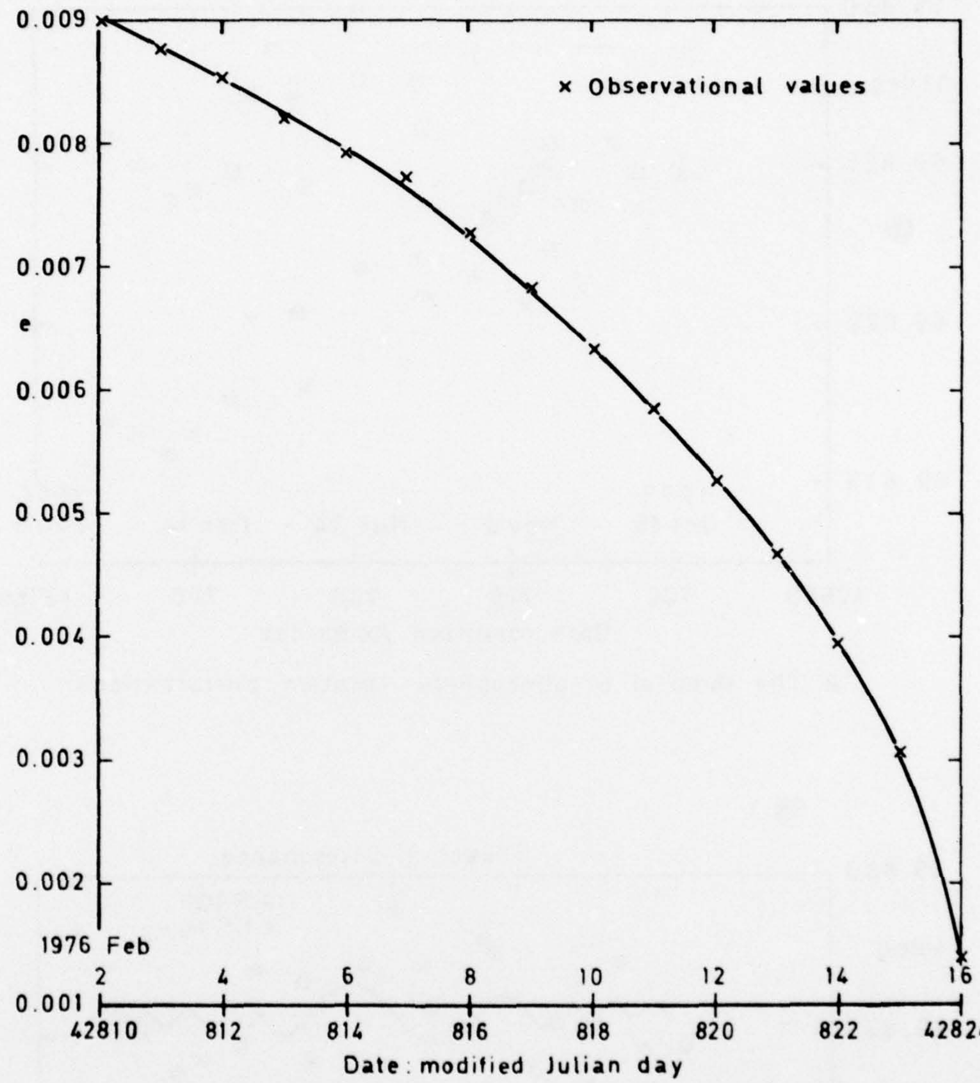

Fig 14 Observational values of eccentricity, near decay

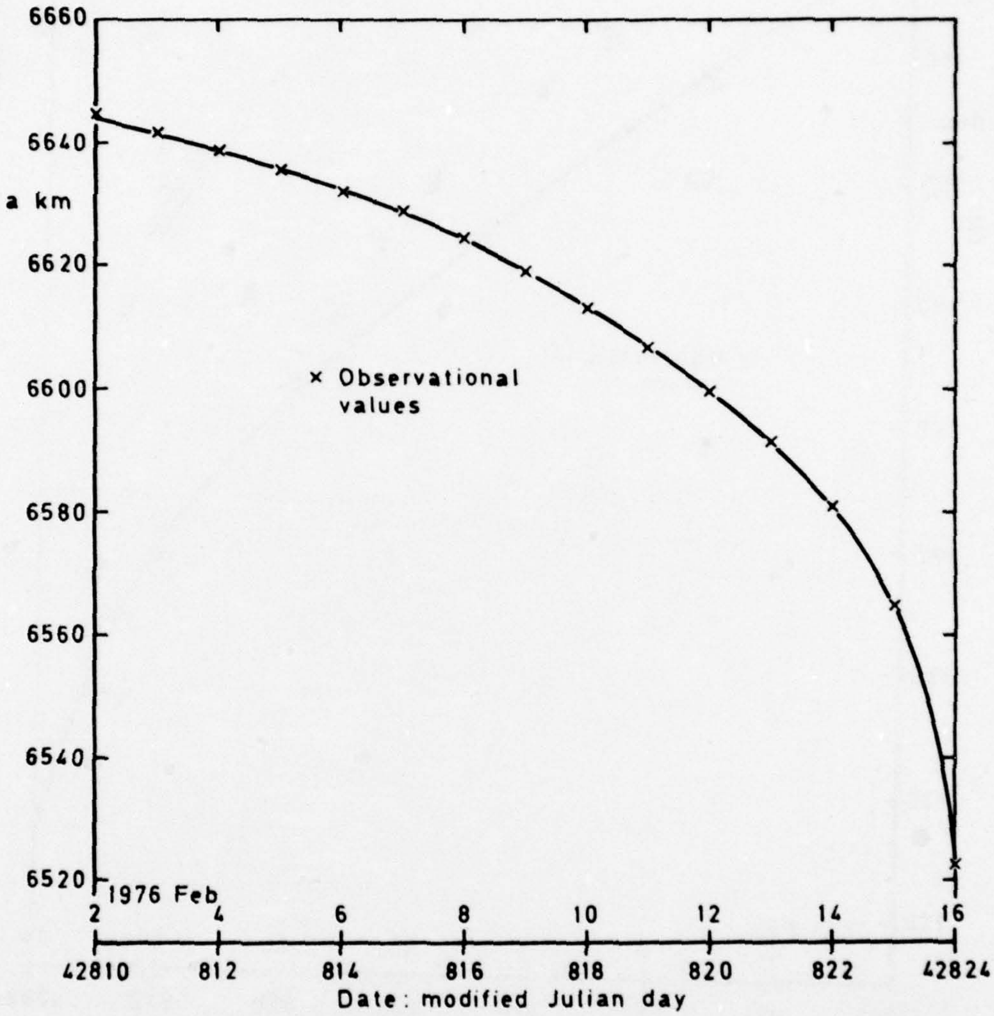

Fig 15 Observational values of semi major axis, near decay

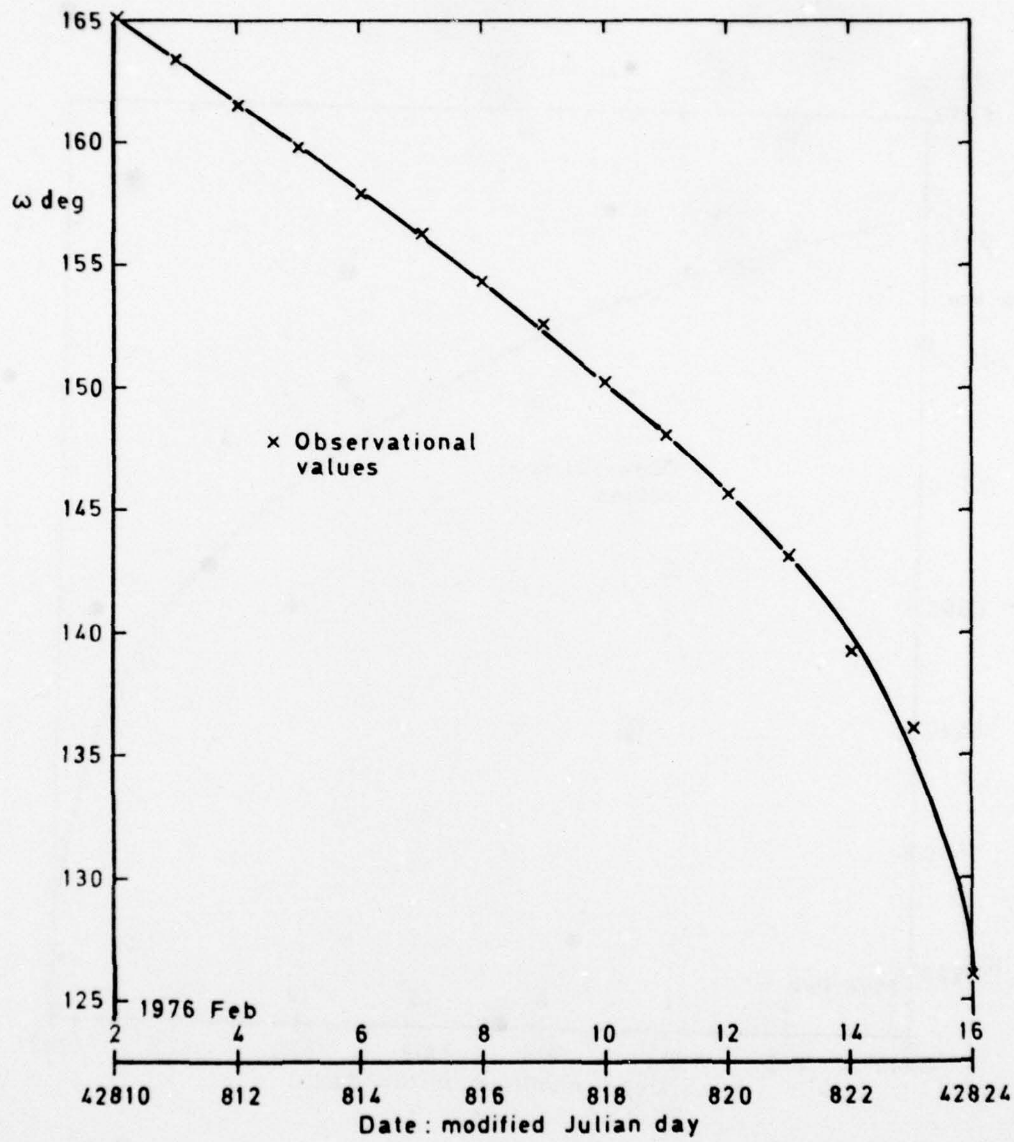

Fig 16 Observational values of argument of perigee, near decay

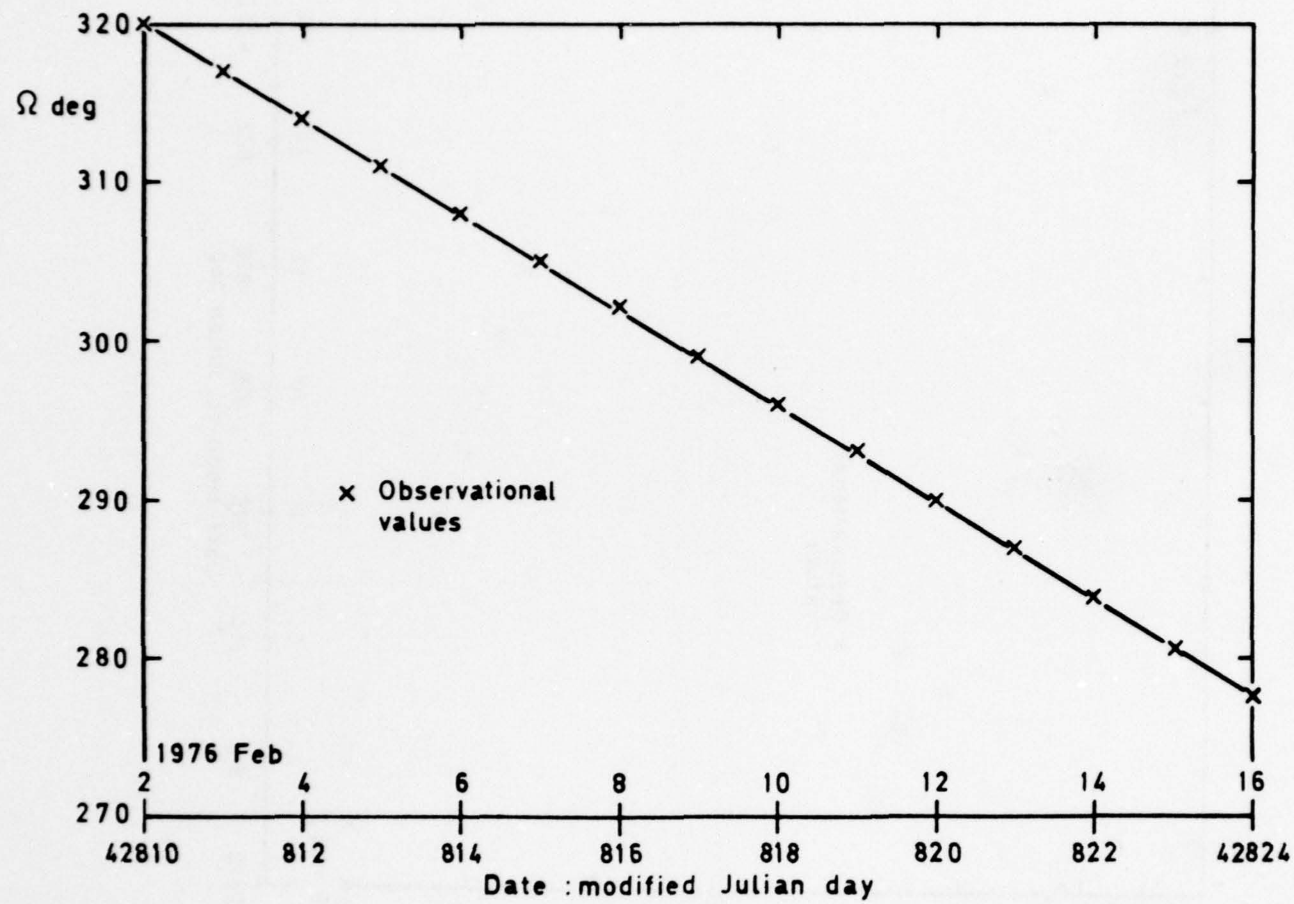

Fig 17 Observational values of right ascension of the ascending node, near decay

Fig 18

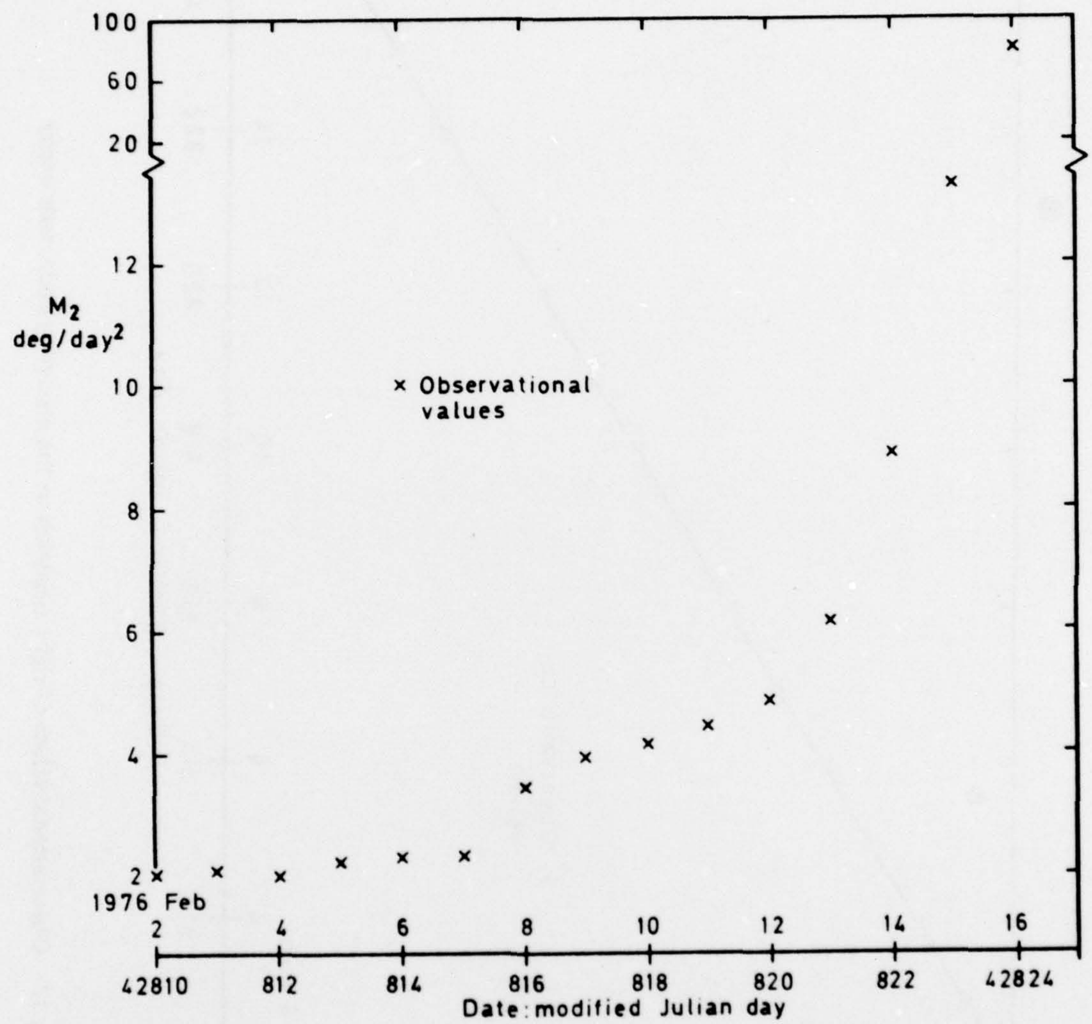

Fig 18 Observational values of orbital decay rate, M_2, near decay

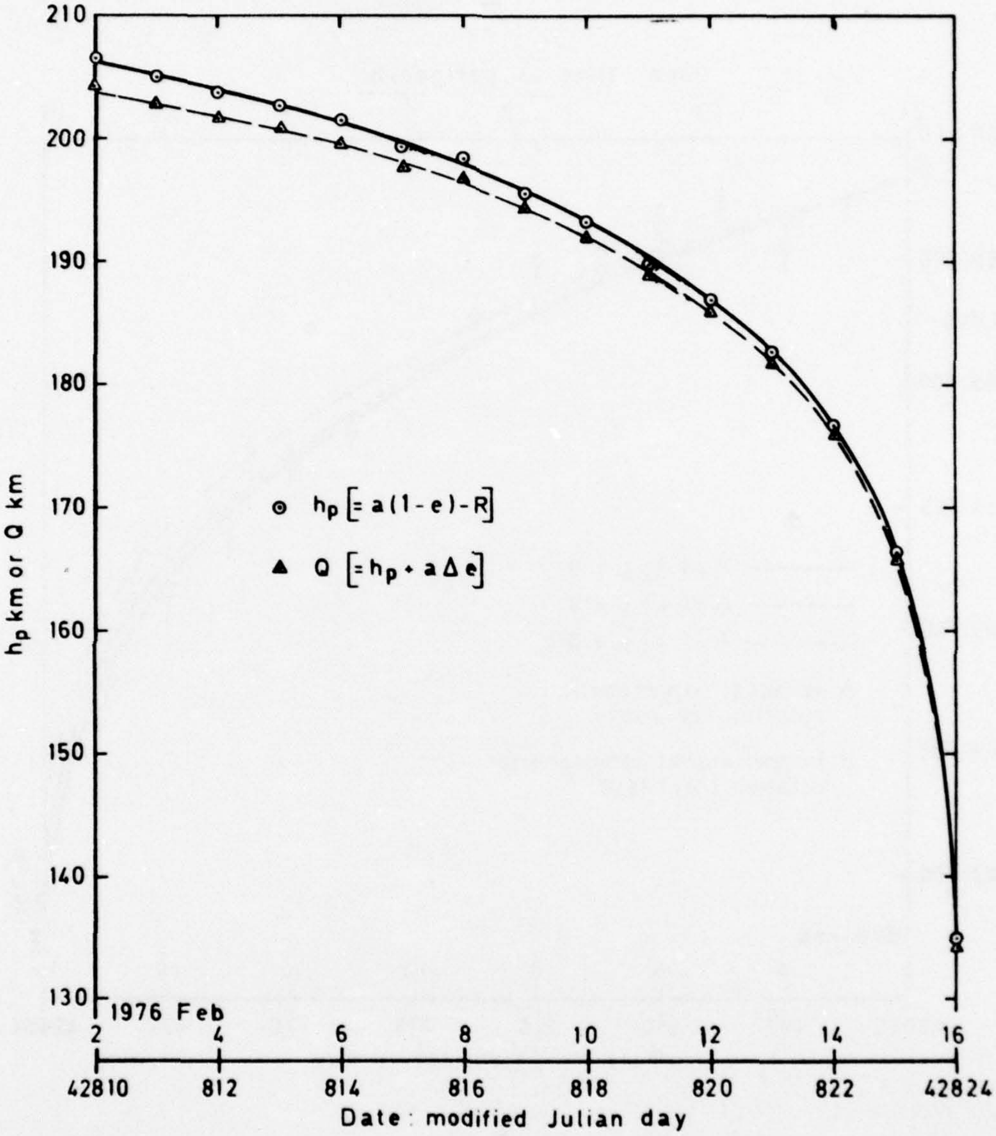

Fig 19 Perigee heights, h_p, and Q (cleared of perturbations), near decay

Fig 20

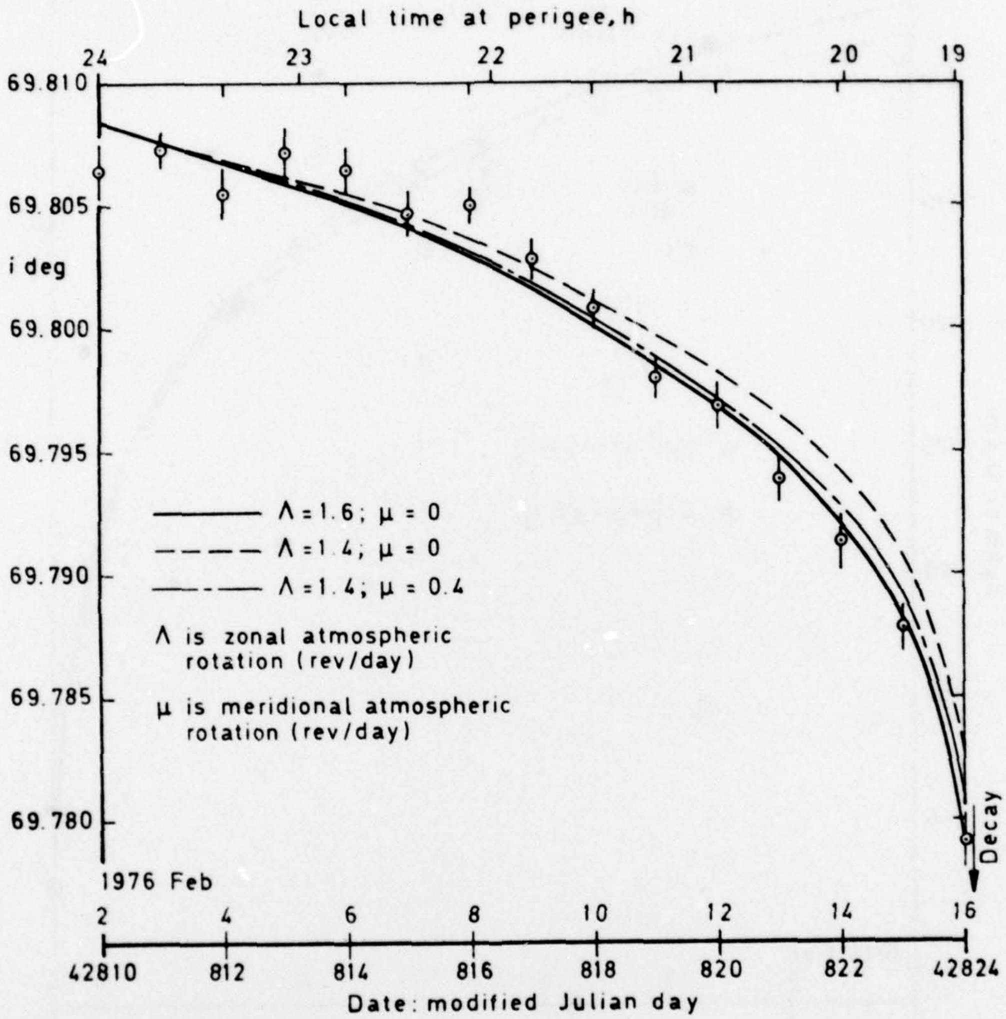

Fig 20 Perturbation-free inclination, with sd, and fitted rotation curves, near decay

REPORT DOCUMENTATION PAGE

Overall security classification of this page

UNCLASSIFIED UNLIMITED

As far as possible this page should contain only unclassified information. If it is necessary to enter classified information, the box above must be marked to indicate the classification, e.g. Restricted, Confidential or Secret.

1. DRIC Reference (to be added by DRIC)	2. Originator's Reference	3. Agency Reference	4. Report Security Classification/Marking
	RAE TR 78107	N/A	UNCLASSIFIED UNLIMITED

5. DRIC Code for Originator	6. Originator (Corporate Author) Name and Location
850100	Royal Aircraft Establishment, Farnborough, Hants, UK

5a. Sponsoring Agency's Code	6a. Sponsoring Agency (Contract Authority) Name and Location
N/A	N/A

7. Title
Determination and geophysical interpretation of the orbit of China 2 rocket (1971-18B)

7a. (For Translations) Title in Foreign Language

7b. (For Conference Papers) Title, Place and Date of Conference

8. Author 1. Surname, Initials	9a. Author 2	9b. Authors 3, 4	10. Date	Pages	Refs.
Hiller, H.			August 1978	48	20

11. Contract Number	12. Period	13. Project	14. Other Reference Nos.
N/A	N/A		Space 557

15. Distribution statement
(a) Controlled by – Head of Space Department
(b) Special limitations (if any) –

16. Descriptors (Keywords) (Descriptors marked * are selected from TEST)
Orbits*. Orbital analysis. China 2 rocket. Rotation rate. Density scale height. Geopotential resonance.

17. Abstract

The orbit of China 2 rocket, 1971-18B, has been determined at 114 epochs throughout its 5-year life, using the RAE orbit refinement program PROP 6, with more than 7000 radar and optical observations from 83 stations.

The rocket passed slowly enough through the resonances 14:1, 29:2, 15:1 and 31:2 to allow lumped geopotential harmonic coefficients to be calculated for each resonance, by least-squares fittings of theoretical curves to the perturbation-free values of inclination and eccentricity.

The rotation rate of the upper atmosphere, at heights near 300 km, was estimated from the decrease in orbital inclination, and values of 1.15, 1.05, 1.10 and 1.05 rev/day were obtained between April 1971 and January 1976. From the variation in perigee height, 25 values of density scale height were calculated, from April 1971 to decay.

A further 1400 observations, made during the final 15 days before decay, were used to determine 15 daily orbits. Analysis of these orbits reveals a very strong west-to-east wind, of 240 ± 40 m/s, at a mean height of 195 km under winter evening conditions.

F5910/1

RAE Form A143